Solvent-Free CO_2 Cycloaddition of Propylene Oxide via Novel Composite of SAPO-34/ZIF-8

by

Hossein Zeinalzadeh

BSc in Chemical Engineering, Sahand University of Technology, 2019, Tabriz

MASTER OF SCIENCE
IN
Natural Resource and Environmental Studies- Environmental Science

UNIVERSITY OF NORTHERN BRITISH COLUMBIA
FEBRUARY 2024

Declaration of Originality and Data Authenticity:

This thesis is a presentation of my original research work. Wherever contributions of others are involved, every effort is made to indicate this clearly, with due acknowledgment of collaborative research and discussions. The work was done under the direct supervision of Dr. Hossein Kazemian at the University of Northern British Columbia (UNBC). I affirm that the data reported herein are authentic, accurate, and represent my work conducted in the laboratory at UNBC. The raw data supporting my findings are preserved in their original form and are available for future reference and verification. This thesis has not been submitted to any other academic institution for the award of any degree or diploma.

Hossein Zeinalzadeh

MSc in Natural Resources and Environmental Studies (NRES)- Environmental Science

University of Northern British Columbia

12/05/2023

Abstract

In this research, ZIF-8/SAPO-34 composites with various wt.% of ZIF-8 and SAPO-34 were prepared and used as catalysts to synthesize cyclic carbonate solventless from CO_2 and propylene oxide. Among composites, SAPO-34/ZIF-8 75:25 wt.% (S/Z25) had the highest conversion value of 92.59%, confirmed by ^{1}HNMR analysis. Various physicochemical techniques were used to characterize the optimized composite, including X-ray diffraction (XRD), SEM, FT-IR, and BET. The impact of different reaction parameters such temperature, reaction time, CO_2 pressure, and catalyst amount on the catalyst reactivity were studied. The highest conversion value has been obtained at 120 psi, 100 ℃, and 240 min. The conversion value was decreased by 20% when the catalyst loading value was changed from 0.4 to 0.1 g. Additionally, the catalyst's recyclability was confirmed for three runs without any significant changes in conversion. However, it was observed that after five repeated tests of reusability, the conversion percentage value decreased from 92.59% to 88.66%.

Keywords: Metal-organic framework, Catalyst, Carbon dioxide conversion, Cyclic carbonates

Graphical Abstract

Through a novel SAPO-34/ZIF-8 composite, the highest CO_2 cycloaddition reaction of propylene oxide to propylene carbonate was achieved at 120 psi, 100 °C, at 240 min.

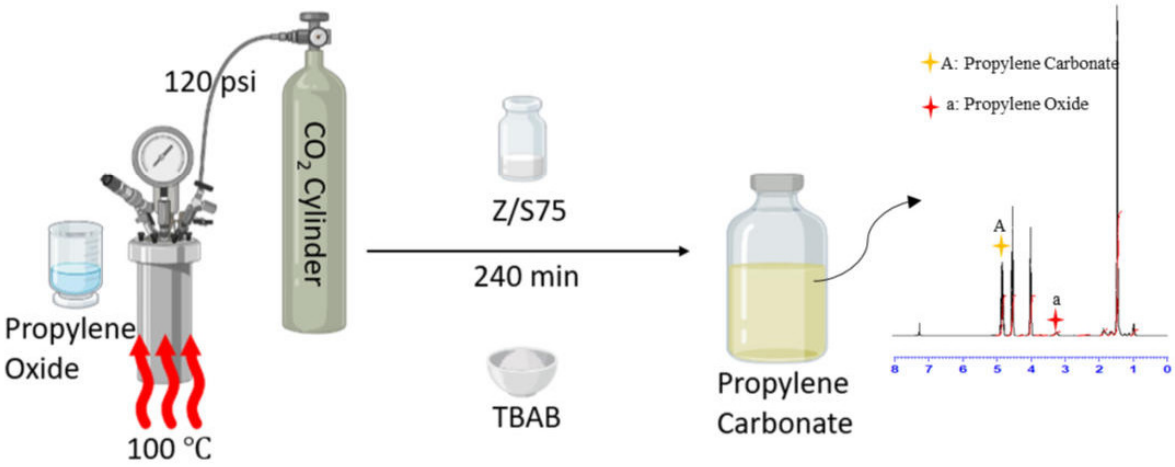

Table of Contents

List of Figures

List of Tables

List of Abbreviations and Symbols

CO_2	Carbon Dioxide
PO	Propylene Oxide
PC	Propylene Carbonate
CH_4	Methane
GHG	Greenhouse Gases
MOF	Metal-Organic Framework
ZIF-8	Zeolite Imidazole Framework-8
SAPO-34	Silico-Alumino-Phosphate-34
MMM	Mixed-matrix Membranes
MCM-41	Mobil Composition of Matter No. 41
SBA-15	Santa Barbara Amorphous-15
HKUST-1	Hong Kong University of Science and Technology-1
MIL-101	Matériaux de l′Institut Lavoisier-101
MSS	Mesoporous Silica Spheres
TEAOH	Tetraethyl Ammonium Hydroxide
TEA	Triethylamine
DEA	Diethylamine
TBAB	Tetrabutyl Ammonium Bromide
TEOS	Tetraethyl Orthosilicate
MTO	Methanol-To-Olefins
KPa	Kilopascal
XRD	X-Ray Diffraction
FT-IR	Fourier Transform Infrared Spectroscopy
SEM	Scanning Electron Microscope
BET	Brunauer-Emmett-Teller
NMR	Nuclear Magnetic Resonance
Ppm	Parts per million
Psi	Pounds Per Square Inch

Acknowledgements

I am grateful to have had the opportunity to work on this thesis, and I am deeply appreciative of the support and guidance I have received throughout this journey.

First and foremost, I would like to express my sincere gratitude to my thesis supervisor, Dr. Hossein Kazemian. His expertise, encouragement, and support have been invaluable in helping me to navigate the challenges of this research project. I am truly grateful for his guidance and mentorship.

Also, I am very thankful to Dr. Hoorieh Jahanbani (Djahaniani) and analytic specialists Charles Bradshaw and Erwin Rehl at the Northern Analytic Laboratory Services (NALS), for their help in the training of characterization and corporation of data analysis. In addition, I am thankful to Mya Schouwenburg, and Dominic Reiffarth for their assistance during my research work. Their insightful feedback, thoughtful discussions, and unwavering belief in me have been a source of inspiration and motivation throughout this process.

I would like to express my appreciation to my family for their unwavering support and love. Their encouragement and belief in me have been a constant source of motivation and inspiration.

Lastly, I would like to acknowledge many individuals who have contributed to this thesis, including my professors, my committee members Dr. R. Thring and Dr. K. Reimer, colleagues and MATTER team members. Without their support and insights, this project would not have been possible.

Thank you all for your invaluable contributions and for being a part of this journey with me.

1. Introduction and Literature Review

1.1 Importance of greenhouse gases processing (Capture, Storage, and Separation)

A rising average air temperature, which is responsible for global warming, has had a significant impact on climatic systems, as well as depleting raw materials and polluting the environment [1]. Climate change has been exacerbated by human activity, which increases heat-trapping greenhouse gases (GHGs) [2]. Due to higher demand in numerous industries, burning fossil fuels for energy production has increased greenhouse gas emissions, contributing significantly to global warming [3]. The COVID-19 pandemic was expected to result in a reduction in CO_2 emissions, but in 2020, atmospheric CO_2 concentrations reached their highest level ever, 412.5 parts per million, which is double what they were at the start of the Industrial Revolution [4].

A variety of approaches can be used to mitigate CO_2 emissions' negative effects. First of all, the use of alternative energy sources, including hydropower, wind power, biomass, and green hydrogen, can be achieved by improving the efficiency of energy conversion techniques, reducing overall energy demand, and enhancing the efficiency of energy conversion techniques [5]. The second way to reduce CO_2 emissions is to replace fossil fuel-based technologies with gaseous fuels [6]. The third solution that can be employed to reduce carbon dioxide emissions is to take the carbon dioxide produced from burning fossil fuels in power plants and industrial processes and store it in appropriate geological formations, depleted petroleum reserves, or the bottom of the sea. A final measure to mitigate CO_2 emissions is to stop deforestation and increase biomass storage [7].

Finally, in order to combat the global warming crisis, it is essential to reduce CO_2 emissions. The reduction of fossil fuel dependence, as well as the storage of carbon dioxide, can be achieved through a variety of approaches [8]. Global warming cannot be mitigated if governments, industries, and individuals do not implement a coordinated global effort to reduce CO_2 emissions [9].

CO_2 has been captured and stored using different technologies in recent decades and can also be converted into precious chemicals and components. Therefore, different methods of capturing and

storing CO_2 are being investigated and implemented, such as post-combustion carbon capture, pre-combustion carbon capture, and oxyfuel combustion systems. Some of the most significant drawbacks of these technologies relate to their separation, purification, compression, transport, and storage procedures. Moreover, CO_2 can be captured using certain adsorbents. Although these materials have some potential for becoming carbon capture and storage technologies, they are being hindered from further development due to the high regeneration temperature and limited CO_2 adsorption capabilities of these materials [8, 10].

It is also possible to convert methane into other components after release through adsorption with solid matter or chemical conversion. There has long been a belief that methane captured by a variety of porous materials can be stored for future or long-distance use as a fuel and that this method is suitable for storing methane. It is therefore necessary to choose adsorbents that have high adsorption and delivery capacities in order to achieve this purpose. According to the United States Department of Energy, the best adsorbent for this application would be one that operates at 315 V(STP)/V with an on-board storage capacity of 0.5 grams of methane per gram of adsorbent, thus allowing a decrease in the amount of methane to be absorbed into the system [11]. Researchers have enhanced existing adsorbents or discovered new ones with excellent properties in order to achieve these objectives. The adsorption of undesirable components such as CO_2 and H_2O tends to be more problematic in methane enrichment and purification than in methane storage systems [12, 13]. Carbon dioxide might be present in an extracted natural gas stream. This is certainly a factor that influences natural gas's heating value and conversion rate. For this application, CO_2 must be separated from a pre-combustion flow with adsorbents with a high affinity for CO_2. Another case study in this report describes the use of dehumidification to remove water from methane streams in order to reduce the formation of methane hydrates and minimize the problems associated with them. This case study also examined the cost-effectiveness of different dehumidification methods, such as the use of membrane technologies and adsorption-based systems. Membrane technologies were found to be the most cost-

effective solution. However, adsorption-based systems were also found to be a viable option in some cases. Ultimately, the right choice of technology depends on the specific characteristics of the pre-combustion flow. The report concluded with an assessment of methane hydrates' impact on the natural gas industry. In both processes, methane is not usually captured but rather is adsorbed, followed by the adsorption of another component during the process of methane separation. Therefore, it is clear that adsorption-based systems are a viable solution for methane separation in certain cases.

Science has made significant advances in the adsorption and separation of gases that explain certain properties of natural selective adsorbents [14]: (I) the surface should be high, as well as the porosity to be desired; (II) the preparation of a low-cost, accessible precursor is fast, easy, and scalable; (III) ability to be shaped into desired structures (beads, monoliths, etc.); (IV) a large amount of gas uptake on both a volumetric and gravimetric basis; (V) high levels of stability under a variety of mechanical, thermal, chemical, and environmental conditions; (VI) superior affinity for the specifically intended molecules in comparison to other gas mixture components; (VII) excellent thermal conductivity; (VIII) the presence of a low-pressure drop within the adsorption bed; and (IX) extremely high cycle stability and high working capacity. These features make adsorbents an attractive choice for various industrial processes. Adsorbents can also be used to purify water and other liquids. Additionally, adsorbents are used in a variety of applications, including air pollution control, water treatment, and energy storage.

A high-rate gas desorption should be provided as part of the adsorption system. This will save energy and allow the system to be more cost-effective. A wide variety of gas mixtures have been studied in the literature for the adsorption and adsorptive separation of methane and carbon dioxide. In the past, mesoporous silica [15], zeolites, porous carbons, and metal–organic frameworks (MOFs) have been discovered as different forms of porous materials [16 ,10]. A wide variety of gas mixtures have been studied in the literature for the adsorption and separation of carbon dioxide from different gas

streams. In the past, mesoporous silica and MOF have been discovered as different forms of porous materials. Many scientists have focused their attention in the last two decades on MOFs, a new generation of materials that is gaining popularity. MOFs have more surface area and a better pore structure than mesoporous silica, making them more effective for adsorption and separation. They are also more selective in the adsorption process, allowing for better gas separation. Additionally, MOFs are less energy intensive. Therefore, there are many advantages to MOFs, including a large specific area, large porosity, and adjustable chemical capabilities that make them an excellent choice for this application [15, 17]. As a result of their unique properties, MOFs have been applied to various spectrums of applications and scales, such as the capture of CO_2 from CO_2/H_2 [39], CO_2/ N_2 [40], and natural gas purification (CO_2/CH_4) [41]. There is still a significant amount of work to be done on developing MOF materials for gas adsorption and separation. More studies must be conducted to improve our understanding of the interactions between MOFs and gases. Additionally, more research is needed to develop more efficient and cost-effective production methods. Finally, more research should be done to optimize the structure and properties of MOFs for their desired applications [18]. The zinc-based MOF CALF-20 has been reported to be highly adsorbent and selective for CO_2 [19]: There is a remarkable difference between the precipitation yields of zeolites and those of the new MOF in terms of space-time. A low amount of water is also adsorbable by CALF-20 at low partial pressures despite its excellent physisorption of CO_2. It is possible to achieve CO_2 capture on an industrial scale by using scalable MOFs. This is because zeolites can only adsorb a certain amount of water before becoming saturated, while MOFs can absorb much more. This means that MOFs can produce much higher levels of precipitation than zeolites, making them more efficient for industrial applications. In addition, MOFs are easier to scale up because they are more flexible and can be produced in large quantities [20].

The term composite material describes a material that has superior properties over other materials in a specific application. In this combination, the merits of the individual components can be retained,

drawbacks can be addressed, and a new composite can be introduced with synergistic effects. In recent years, many researchers have specifically considered MOF-based composite materials in addition to extensive studies of MOF materials in greenhouse gas treatment. Composite materials made from MOFs have a continuous phase or a distributed phase. MOFs can typically be used in combination with other components, like graphene-based materials, as a layered medium for other constituents, while in a distributed one, the MOF particles can be incorporated with other components, as in the MOF/zeolite composite, or dispersed in a continuous phase of polymer like in mixed matrix membranes (MMM) [21]. MOFs' added composition determines their performance in the adsorption and separation processes based on their type and content. In addition, MOF materials often have some shortcomings that make them unsuitable for many applications, such as their relatively weak bonding between metallic nodes and organic ligands, poor handling properties, and moisture sensitivity. This makes them difficult to use in many applications that require strong bonding, long-term stability, and resistance to moisture [22]. It is possible to develop an enhanced adsorbent by hybridizing MOF materials with a suitable component, achieving synergistic effects and/or developing new properties, and extending the use of MOF materials to new areas by hybridizing them with a suitable component. MOFs can be improved by combining them with composites to improve their chemical stability and thermal conductivity. MOFs can also be used in energy systems by using composites, which will solve their electronic conductivity problem. This is because composites make the MOFs more stable and conductive, allowing them to be used in a wider range of applications. In particular, well-designed MOF-based composites can also improve the adsorption characteristics needed for gas storage, separation, and catalysis applications. Solar cells that produce renewable energy can also be improved with MOF-based composites. Due to their ability to absorb and convert more sunlight, composites can improve solar energy conversion efficiency. As well as improving the efficiency and safety of fuel cells, MOF-based composites are also capable of reducing fossil fuel dependence and increasing electricity generation. By combining

the MOFs, denser atomic structure and stronger dispersive forces between the guest molecules are achievable. Also, MOF composites are able to catalyze and adsorb more effectively due to their hierarchically porous structure. By comparing MOF-based composites with pristine MOFs, these can demonstrate their utility in a variety of applications. Several MOF-based composite materials have been developed, including MOF/Si, MOF/C, and MOF/metal oxide. These composite materials offer a number of advantages over traditional MOFs, such as increased surface area and porosity, improved thermal and chemical stability, and greater binding affinity. Additionally, they can also provide more efficient separation of guest molecules and can be tailored to specific applications. Some of the main characteristics of the compounded materials with MOFs and some typical composites are listed in Table.1.

A MOF-based composite material's performance is closely related to the bonding between the MOF and other components [23]. A composite membrane fabricated from MOF-based MMM composites can be selectively separated and stabilized based on the interfacial bonds formed between the MOF particles and the continuous polymeric phase [24]. In addition, the negative effects of hydrogen bonding between graphite oxide oxygen atoms and copper atoms in MOF structures could lead to structural defects [25].

In recent times, there has been a significant surge in interest surrounding MOF-based composites, particularly in the context of methane and carbon dioxide treatment. Recent research has unveiled noteworthy breakthroughs in the utilization of MOF materials across various adsorption and separation processes [26-28], the synthesis of core–shell MOF composites for different applications [29], MOF/Mixed Matrix Membrane composites for the CO_2 separation [30], MOF-composites for CO_2 capture [31], and gas adsorptions/separations using MOF/polymer composite membranes [32] and some MOF/graphene hybrids [33]. Only a small number of studies have explored the adsorption and selective separation of CO_2 using MOF-based composite materials. The present study reports on the development of a novel class of MOF-based composites (MOF/Zeolite composites). This results

in the creation of a hybrid adsorbent with enhanced structure and improved characteristics, leading to increased adsorption capacity and/or greater selectivity in gas separation. In this context, the silica component can either be a crystalline silicate or an amorphous silica molecular sieve possessing the required structural and surface properties. This study primarily emphasizes the use of silica-based materials in conjunction with MOF for the adsorption and separation of greenhouse gases.

1.1.1 MOF/Zeolite-based Composite Materials

Zeolites are aluminum silicates that can be used to adsorb and separate GHG gases. They are one of the most important and fascinating compounds that have attracted attention. The resultant composites may be seen in a variety of forms, as the result of pristine materials and synthesis approaches being used, including core-shell particles, zeolite particles decorated with MOF layers, and supported MOF layers with zeolite plates. It has become possible to develop new selective adsorbents based on MOF/Zeolite composites that offer enhanced characteristics over the individual MOF and zeolite components they replace.

Recent years have seen an increase in the use of MOF/Zeolite composites due to the fact that they have a higher specific surface area and pore volume as compared with the parent MOFs. As an example, Al-Naddaf et al. [34] investigated the adsorptive behavior of methane and carbon dioxide using zeolite-5A@MOF-74 core–shell composites developed by seeded growth. A composite consisting of 5 and 95 wt.% zeolite core and shell, respectively, revealed that this composite, when compared with the parent constituents, has a greater porosity, with a 29% increase in the pore volume and a 27% increase in the surface area compared with the parent constituents. Physisorption experiments carried out with N_2 were found to have improved the N_2 physisorption efficiency, and this was attributed to the creation of new mesopores at the interface between the MOF and the zeolite. The zeolite-5A@MOF-74 composite with 5 wt.% zeolite content has a surface area of 1504 m^2/g and a mesoporous volume of 0.15 cm^3/g compared to the parent adsorbents, which have a surface area and porosity much lower than those of Zeo-A@MOF-74–1. A hybrid compound containing zeolite,

depending on the weight fraction of zeolite, was observed to be capable of adsorption more CH_4 and CO_2 than its pristine constituents depending on the zeolite percentage. [35, 36]. Compared with a lone MOF, both gases adsorb more efficiently on a composite containing 5 wt.% zeolite. The CO_2 and CH_4 adsorption capacities of Zeo-A@MOF-74-1 were remarkable at approximately 1 bar and 25 °C (7 and 1 mmol/g, respectively). The adsorption properties of this composite have been shown to be suitable for hydrogen separation applications, in particular the purification of out-stream in steam methane reformers, because of the negligible amount of hydrogen that is observed in its adsorption and its very high selection of gas over hydrogen. Furthermore, the composite is stable and can withstand high temperatures and pressures, making it ideal for hydrogen separation applications. Additionally, Zeo-A@MOF-74-1 is relatively inexpensive and can be easily synthesized in large quantities. For the composite to achieve maximum separation and adsorption efficiency, it was recommended that the weight ratio of zeolite to MOF be optimized. The selective amounts estimated in this study have been predicated on adsorption isotherm data for a single gas, which have proved to be very useful in estimating the selectivity amounts. The authors evaluated the isotherms of corresponding gases at higher pressures, similar to those found in industrial environments, and found that the uptake of methane was 17% higher than that of MOF-74 when exposed to 20 bar, which is comparable to the uptake of methane under the same conditions at 20 bar. This suggests that the adsorption isotherm data for a single gas can provide a good indication of the selectivity amounts when the gas is exposed to higher pressure, such as those found in industrial environments [37].

The emissions released by various industries often contain H^2O, which, despite being a common component of exhaust gases, also contributes to the greenhouse effect. As a result, it gives scientists the chance to work on synthesizing hydrophobic adsorbents. Hydrophobic adsorbents are materials that can be used to separate other gases, such as CO_2, in the presence of H_2O vapor. The recovered H2O can subsequently be repurposed for various applications, including energy production.

In an eco-friendly approach, Yang et al. [38] combined LiX as a core and ZIF-8 as a hydrophobic shell to create LiX@ZIF-8 as a novel composite. An ion exchange technique was used to create LiX by exchanging Li^+ with 13X zeolite. ZIF-based core–shell produced with these modifications were more stable and hydrophobic. A comparison of 13X zeolite and ZIF-8 hydrophobic properties revealed that LiX@ZIF-8 had neutral hydrophobic properties. A 50% relative humidity (RH) leads to a significant improvement in CO_2 adsorption efficiency. New composites were evaluated in terms of their CO_2 adsorption capacity and cycle stability using a dynamic experimental system. This study evaluated the performance of LiX@ZIF-8-I as monolayers in flue gas with a high level of humidity, thus indicating that it showed a significant improvement for CO_2 capture, with a potential improvement of 1.73 mmol/g, when compared to the results of characterization and dynamic adsorption.

Tate et al. [39] constructed MOF/zeolite composites in the same way the core-shell structure was developed, using zeolite-5 beads covered with different coordinating metal MOF layers. The adsorption performance of the nanovalved 2-layer MOF composites was increased in the order of Cu < Co < Ga < Al. There were differences in layer morphology, uniformity, crystal intergrowth, and cracks that contributed to this difference. The layers were thicker in the high-temperature samples, and the layers had less crystal intergrowth and cracks compared to the low-temperature samples. Furthermore, their studies showed an increase in methane storage capacity was achieved by crystallizing MOF on zeolite surfaces in two steps. There are also a number of composites consisting of MOF and zeolite-based composites for CO_2 adsorption and separation which are presented in Table 1.

Table 1: MOF/Silica-Based Composite Materials in Adsorption/Separation of CH_4 and CO_2 Greenhouse Gases [40]

MOF composite	adsorption conditions	quantity adsorbed CO_2	selectivity (α)	application	Ref.
MOF-74/zeolite-5A	25 °C 1 bar	~7 mmol/g	CO_2/H_2 (50/50): 8659	H_2 purification	[34]
MOF-74/zeolite-5A	25 °C 20 bar	13.8 mmol/g	CO_2/H_2 (15/85): ~250		
HKUST-1/MCM-41	30 °C 4 bar	2 mmol/g	CO_2/CH_4: 5.7	CO_2/CH_4 separation	[41]
ZIF-8/zeolite-5A	25 °C 1 bar	2.61 mmol/g	CO_2/H_2O: 6.61	CO_2 capture in presence of water	[42]
ZIF-95/zeolite-4A	0 °C 1 bar	~22.5 cm^3/g	CO_2/CH_4 ~ 24.6	CO_2/CH_4 separation	[43]

1.1.2 MOF/Non-Zeolitic Silica Composites

These composites also contain a variety of silica-based materials in addition to the MOF/zeolite hybrids. The adsorption and/or separation of methane and carbon dioxide has also been studied using MOF composites containing non-zeolitic silica materials, such as MCM-41, SBA-15, and aminoclay. The MCM-41 material belongs to the M41S family of mesoporous silicas. There are a number of advantages in using honeycomb-ordered porous silica material for research purposes. In the functionalized form [44, 45] or the composite structure [46], this porous silica material has an orderly honeycomb structure, adjustable pore size distribution, and high porosity. Also, Tari et al. were able to separate CO_2/CH_4 using MCM-41 composite with MOF when the matrix phase used was MOF(Cu)/Si as the compound [41]. A microwave-assisted synthesis procedure was employed in this study to embed HKUST-1 MOF into MCM-41's hexagonal channels. According to the results, the growth of HKUST-1 particles in the MCM-41 matrix enhanced the selective adsorption of CO_2 over methane as well as the structural properties of the system. Copper salt's molar ratio to matrix in the

composite in the preparation played a role in this enhancement. A study carried out by this group further developed the MCM-41 matrix by functionalizing it with -COOH prior to the formation of MOF in the channel [47]. A wide range of pressures were examined again while comparing the resultant composite to the MOF and MCM matrix in its pristine form and the resultant composite showed a significant increase in CO_2 selectivity over methane.

According to Dr. Chen's research, another study [48] has been conducted to evaluate the efficiency of CO_2 capture in MIL-101(Cr)/mesoporous silica with the help of this composite. Based on what the authors have found out, there appears to be a connection between Cr^{3+} in MIL-101(Cr) and the hydroxyl group in silica-based materials (MCM-41) in this study. In order to investigate the CO_2 capture capacity of both pristine MIL-101(Cr) and MCM-41 as well as the chemical mixture of both samples, a synthetic composite was compared with both samples at pressures ranging from 0 – 100 KPa and temperatures ranging from 25, 35, and 45 ℃. It was found that at 25 ℃ and 1 bar, the best level of CO_2 capture was achieved. On the other hand, the composite was used to evaluate the selectivity that could be achieved in a gas mixture consisting of 15%–85% CO_2 compared to N_2. The composite was also studied for its reusability. A vacuum oven at 373 K was used to test the CO_2 desorption capacity between each of the eight CO_2 capture cycles. Based on the results of the experiments, it has been shown that the CO_2 adsorption rate was comparable in each cycle.

It has been reported that Sorribas et al. [49] have successfully fabricated hierarchically porous MCM-41/ZIF-8 composite materials from MCM-41/ZIF-8. Also, a mesoporous silica-NH_2-MIL-53(Al) core-shell sphere was synthesized for the purposes of CO_2 uptake in another. NH_2-MIL-53(Al) crystals were seeded into mesoporous silica spheres (MSSs) to become MCM-41 particles. The second step was to make a MOF shell by growing secondary crystals.

Additionally, the adsorption capacity of CO_2 was studied with a composite core-shell. The MSS-NH_2-MIL-53(Al) and MSSs have been found to be very effective CO_2 adsorbents, with CO_2 adsorption capacities of approximately 2 and 1 mmol/g, respectively, at a pressure of 1 bar. A further

important factor is the high pressures that MSSs were applied at, exceeding 3.0 MPa at the time. In this study, CO_2 adsorption was positively affected by a change in pressure. There was a significant increase in the amount of CO_2 absorbed by the cells, and it reached 16 mmol/g. In this research, both NH_2-MIL-53-(Al) and MSS-NH_2-MIL-53(Al) demonstrated comparable adsorption capacities, reaching approximately 10 mmol/g at a CO_2 partial pressure of nearly 3.5 MPa. This observation stems from the effective CO_2 capacity of the core–shell particle, attributed to its silica mesoporosity. Because the MSSs lose some porosity during MOF synthesis, the overall adsorption value is a bit lower than expected based on individual contributions (19 wt.% MSSs and 81 wt.% MOFs) [49].

As part of the gas adsorption/separation process, silica materials such as aminoclay have also been considered in combination with MOFs. A layered aminoclay and ZIF-8 self-assembled composite was demonstrated for the first time by Chakraborty in 2017 [50]. A comparison was made between ZIF-8/aminoclay composites and pure ZIF-8 and a significant improvement was found in the adsorption capacity of the composites. In order to fabricate the four different types of composites, the authors altered the clay content to produce four different types: ZIF-8/aminoclay-1, ZIF-8/aminoclay-2, ZIF-8/aminoclay-3, and ZIF-8/aminoclay-4. Based on the results of the analysis, it has been determined that the aminoclay content of the mentioned materials is respectively 12.1, 18.3, 22.2, and 27.2%. In the first attempt at developing new composites, MOF nanoparticle assemblies with functional materials were combined. The purpose of this study was to study the CO_2 and N_2 capacities of the labeled composites so that they could measure the performance of the composites. Accordingly, based on the BET & CO_2 isotherm analysis, the synthesized composites were found to have a higher storage capacity when compared with the pure ZIF-8. During the creation of the nanoparticles, the number of effective neighboring framework atoms, which can be used to boost adsorption capacity, increased as a result of a raise in the effective number of neighboring framework atoms. Further, the researchers discovered that amine groups in the composite act as binding sites for CO_2 molecules, resulting in a higher level of adsorption and absorption of CO_2, as demonstrated by

in situ Raman measurements performed on one of the composites in the presence of CO_2. Experiments were conducted to confirm this theory. 25 °C and 0–1 bar was used to operate the CO_2 adsorption isotherms on the samples. Although the pristine aminoclay did not have a high adsorption capacity, it was observed that the composite ZIF-8/aminoclay-2, which was prepared by adding 18.3 weight percent or aminoclay to ZIF-8, showed an impressive adsorption capacity (i.e., 31.9 mL/g at 1 bar) compared with the pure aminoclay. There was a notable increase in the BET of ZIF-8/aminoclay-2, which was 1461 m^2/g after the addition of aminoclay to ZIF-8, which resulted in a higher BET for ZIF-8/aminoclay-2.

In order to solve the problem, it might be necessary to improve the hydrophobicity of the sorbent material. The carbon capture process could also be improved by developing new materials that are more moisture resistant or by exploring new techniques to ensure that moisture does not interfere with the process of carbon capture [51].

1.1.3 CO_2 Conversion

Several industrial processes incorporate CO_2 as a fundamental element. However, due to the highly oxidized nature of CO_2, its low energy level presents a significant challenge in developing industrial procedures based on CO_2 as a raw material [52-55]. Consequently, substantial energy input is necessary to convert CO_2. One potential solution is to use high-energy starting materials like hydrogen, unsaturated compounds, small-membered ring compounds, and organometallics to facilitate the conversion process. Another approach is to select oxidized low-energy synthetic targets such as organic carbonates. Furthermore, the elimination of specific chemicals can shift the equilibrium towards the product side, leading to efficient CO_2 conversion. Alternatively, energy in the form of light or electricity can be supplied to provide the necessary energy input for the conversion process. Further research in these areas could enhance the efficiency and practicality of CO_2-based industrial processes [56, 57].

1.1.4 Cyclic Carbonates

The utilization of CO_2 as a raw material in industrial processes has been proposed as a promising approach for reducing carbon emissions and combating climate change. CO_2 is the most oxidized form of carbon and has a low energy level, which makes constructing industrial processes based on CO_2 challenging [58]. However, the reuse of CO_2 is a preferable alternative, which compensates for the cost of the collection stage, the most energetically demanding part of the entire cycle. Several processes that employ CO_2 as a feedstock or reaction medium have been reported in the literature. However, most of these processes demand high-purity CO_2, which increases the cost of the separation process. Therefore, combining CO_2 extraction and recycling in a single stage is a more feasible approach. The synthesis of cyclic carbonates by CO_2 cycloaddition is one of the most promising methods for CO_2 fixation. Cycloaddition of CO_2 to epoxides is the most common and effective way to prepare cyclic carbonates as an industrial process [59, 60]. This reaction is advantageous for green and sustainable chemistry because it uses carbon dioxide, a renewable and widely available reactant that exhibits 100% atom efficiency. Furthermore, this reaction can be conducted without solvents effectively. To counterbalance the high thermodynamic stability of carbon dioxide, the reaction exploits the free energy of epoxides. Propylene carbonate and ethylene carbonate, prepared from propylene oxide and ethylene oxide, respectively, are the most commonly synthesized cyclic carbonates, as they are efficient in balancing the thermodynamics of the reaction. In conclusion, the reuse of CO_2 in industrial processes, especially in the synthesis of cyclic carbonates, holds immense potential for sustainable and green chemistry practices [61].

Propylene carbonate is a highly versatile chemical that finds widespread application in various industries. It is a cyclic carbonate that serves as a safer alternative to several hazardous organic solvents such as dimethylformamide, hexamethylphosphoramide, N-methyl-2-pyrrolidone, dimethylacetamide, and acetonitrile. Due to its unique properties, propylene carbonate has been utilized in various industrial processes such as solvent extraction, electrolyte in lithium-ion batteries,

and as a solvent for chemical reactions. Propylene carbonate has a low toxicity profile, making it an attractive option for industries seeking to minimize their environmental impact [62].

1.1.5 Propylene Carbonates

Propylene carbonate is a polar aprotic solvent that possesses several advantageous properties such as high dielectric constant, large temperature range (liquid at atmospheric pressure between −49 and 242 °C), low viscosity, colorlessness, and odor lessness. In terms of health and safety, it is a safe solvent with low vapor pressure, low toxicity, low flammability (high flash point), and no corrosiveness [63, 64]. Moreover, propylene carbonate is biodegradable in both air and water, where it hydrolyses slowly to yield low-toxicity products such as propylene glycol and carbon dioxide [65]. Due to these properties, propylene carbonate is considered a highly sustainable and green solvent by various regulatory agencies [66]. However, determining the metrics for evaluating a green solvent is a challenging task that requires making certain assumptions, leading to discrepancies in the ranking of propylene carbonate. The CHEM21 Selection Guide [67], for instance, identifies propylene carbonate as problematic, mostly due to its high boiling point, which necessitates energy-intensive distillation under reduced pressure for solvent recovery and recycling.

1.2 Catalysis

1.2.1 Why Catalysts for CO_2 gas conversion?

The reactivity of different epoxides in the cycloaddition of CO_2 varies, but a catalyst is necessary for the reaction to proceed at acceptable rates. The nature of the catalyst, in combination with the nature of the epoxide and reaction conditions, is crucial in determining selectivity between the two potential products, cyclic carbonates and polycarbonates [68]. Lewis's acid sites can coordinate with the epoxide O atom are the most common and active catalytic systems for this reaction. MOFs and Zeolitic imidazole frameworks (ZIFs), two subclasses of porous materials, are promising candidates for both CO_2 capture and catalysis application. However, most MOFs and ZIFs are unstable in the

presence of water, which is a significant challenge in many industrial applications [69]. SAPO-34 materials are practical laboratory zeolites that can be used for carbon dioxide capturing and conversion, as they can overcome the limitations of MOFs and ZIFs. Although porous materials are effective for CO_2 capture and conversion, their high cost is a significant drawback [70].

Studies have shown that the use of heterogeneous catalysts provides an efficient and practical solution for CO_2 capture and conversion. The immobilization of catalysts onto porous materials, such as MOFs and ZIFs, enhances their performance by providing a defined pore structure and available acid sites. Among these materials, MOFs have become increasingly popular due to their exceptional chemical and physical properties. MOFs have a high specific surface area, well-defined pore structure, and adjustable functionality, making them ideal candidates for gas separation and catalytic applications. However, most MOFs suffer from poor stability under humid conditions, which limits their use in industrial applications [71, 72].

To overcome this limitation, scientists have been developing hydrophobic MOFs and ZIFs with superior stability against humidity. One promising candidate is SAPO-34, a practical laboratory zeolite that can overcome the limitations of MOFs and ZIFs. SAPO-34 has a well-defined pore structure and exceptional thermal and chemical stability, making it an attractive option for CO_2 capture and conversion [73]. Despite their effectiveness, porous materials' high cost remains a significant drawback for their commercialization. To address this issue, researchers have been exploring alternative materials that can provide comparable performance at a lower cost. One such alternative is zeolites, which are commercially produced and have been used in various applications, including CO_2 capture and catalysis [74].

1.2.2 MOFs as a novel catalyst for CO_2 gas conversion

MOFs are a group of hybrid materials that are gaining popularity in scientific research due to their unique properties, such as high specific surface area, adjustable pore size distribution, and surface chemistry [75]. These features make MOFs particularly attractive for a range of applications, including gas and liquid capture and separation, heterogeneous catalysis, sensing, and drug delivery. In recent studies, MOFs have been explored as a promising material for CO_2 reduction [76]. Nathaniel L. Rosi and colleagues [77] investigated the crystal structures of MOF-69A−C and MOF-70−80, which enabled the design and construction of porous structures. Similarly, Wen-Yang Gao and colleagues synthesized MOF-505 and demonstrated its high catalytic activity in the chemical fixation of CO_2 into cyclic carbonates at room temperature and under 1 atm pressure [78]. MOFs' porous structures, which are constructed from discrete metal carboxylate clusters and organic links, can be systematically varied in pore size and functionality. This allows for the synthesis of MOFs with extraordinary properties that can be tailored for specific applications [79].

Furthermore, researchers have been exploring various strategies to enhance MOFs' performance in CO_2 reduction [80]. For instance, MOFs' catalytic activity can be improved by introducing metal nanoparticles within the porous structures, which enhances the adsorption of CO_2 and promotes its conversion into valuable products. Additionally, the introduction of co-catalysts, such as metal oxides, can further enhance the catalytic activity of MOFs in CO_2 reduction reactions [81]. Moreover, the use of MOFs in CO_2 capture and storage has been extensively studied, and numerous studies have reported their high efficiency and selectivity in capturing CO_2 from gas mixtures. As the world faces an impending climate crisis, MOFs' potential for CO_2 reduction and capture provides a promising avenue for addressing global carbon emissions [82].

Special subclasses of MOFs are ZIFs, which are constructed from tetrahedral single-metal nodes and imidazole-based linkers. This combination of constituents results in tetrahedral structures that resemble those found in inorganic zeolites [83]. Consequently, ZIF structures feature large cages that are connected through narrow windows, and they possess high thermal and chemical stability. Future

research will explore the potential of ZIFs for various applications, such as gas and liquid adsorption, separation, and catalysis. Moreover, the systematic variation of the pore size and functionality of ZIFs could yield new materials with tailored properties and enhanced performance. Therefore, the design and synthesis of MOFs, including ZIFs, holds great promise for the development of novel materials with diverse applications in various fields [84].

The strong interaction between the charged imidazolate linkers and the metal ions, in combination with the preference for the formation of rigid cages, makes ZIFs highly resistant to mechanical, thermal and chemical stresses, setting them apart from classic coordination networks [85]. ZIFs possess a zeolite-like structure, wherein tetrahedral nodes are connected by bent organic linkers to form a 3D porous network with a narrow pore size distribution [86]. The unique combination of tetrahedral nodes and bent linkers results in ZIFs having an angle (M-imidazolate-M) of approximately 145°, which is very similar to that observed in zeolites for the angle ∠ (Si-O-Si). This similarity in the structural motif between ZIFs and zeolites makes ZIFs highly attractive materials for a range of applications, including gas adsorption, separation, and catalysis. Recent studies have explored the design and synthesis of new ZIFs with tailored properties by introducing functional groups into the imidazolate linker or by using different metal ions as nodes [87, 88]. Such approaches offer a promising avenue for tuning the pore size, shape, and functionality of ZIFs to meet specific applications' requirements. Additionally, the use of ZIFs in combination with other materials, such as polymers or metal nanoparticles, can further enhance their performance in various applications, including sensing and drug delivery [89]. The potential for ZIFs in various fields underscores the importance of further exploring their unique structural features and the factors that influence their properties to design and synthesize highly optimized ZIFs with tailored properties for specific applications [90].

The coordination chemistry of metal-imidazolate and the corner-sharing SiO_4 tetrahedral has paved the way for the synthesis of numerous ZIF topologies, with over 100 structures identified to date.

Traditional hydrothermal and solvothermal synthesis routines have been used to prepare ZIF materials at varying temperatures and reaction times. However, as the field of ZIF synthesis continues to progress, new strategies have been developed to address limitations associated with traditional methods [91]. Solvent-based and solvent-free methods have been found to be effective in preparing ZIF-based materials. Moreover, novel synthesis approaches, such as microwave-assisted, electrochemical, and mechanochemical synthesis, have been developed to improve the efficiency and scalability of ZIF synthesis [92]. These diverse synthesis strategies have significantly expanded the range of ZIF-based materials that can be produced and have opened up new avenues for exploring their potential applications in areas such as gas storage, separation, catalysis, and drug delivery [93].

1.2.3 silicoaluminophosphates (SAPO) as a novel catalyst for CO_2 gas conversion

The unique chemical structure, pore size distribution, and thermal, chemical, and ion exchange properties of silicoaluminophosphate (SAPO) zeolitic materials have gained significant research interest, setting them apart from other commonly used zeolites . Various catalysts, such as ionic liquids, quaternary ammonium salts, metal oxides, and metal complexes, have been employed to synthesize cyclic carbonates through the cycloaddition of CO_2 to epoxides [94]. SAPO crystals are microporous and contain silicon atoms, which replace some of the aluminum and phosphorus atoms. The cavity structures of some SAPOs have dimensions equivalent to the kinetic diameters of molecules such as CO_2, CH_4, N_2, and O_2 . This unique feature of SAPOs may enable them to be used for CO_2 capture from natural or flue gas and/or conversion of CO_2 into valuable chemicals, opening up a range of potential applications [95].

In 2017, Ahmed and a colleague published a research article that explored the potential of SAPO-34 as a catalyst in the synthesis of cyclic carbonates from epoxides by activating and utilizing CO_2 [96]. In addition, it has been reported by Xie et.al that SAPO-56 shows high efficiency as a catalyst in the transformation of CO_2 into cyclic carbonate. The exceptional capability of SAPOs to adsorb CO_2

along with the existence of Bronsted acid sites linked with Al ions and Lewis acid sites associated with OH groups provides evidence to support the feasibility of utilizing this material for this purpose [97]. SAPOs possess a three-dimensional framework of Silicoaluminophosphates, where well-defined TO_4 cavities or channels of molecular sizes connect to their neighbors through corner sharing. Although there are 239 approved framework type codes by the International Zeolite Association- Structure Committee (IZA-SC), only a limited number of SAPO forms have been synthesized for acid catalysis. Based on the number of T atoms in the pore opening, SAPO MSs can be categorized into small (8 T), medium (10 T), large (12 T), and extra-large pores (>12 T) [98]. SAPO-34, a Silicoaluminophosphate with a small pore size, has been widely studied for its potential in various research applications. The use of a template in the synthesis of zeolites plays a critical role in determining the structure of the pores and cages. In the case of SAPO-34, it can be synthesized using various organic amines as templates, including tetraethylammonium hydroxide (TEAOH), dipropylamine, isopropylamine, piperidine, morpholine, triethylamine (TEA), and diethylamine (DEA), among others. Hydrothermal synthesis is the most commonly employed method for preparing this type of catalyst, with the template type and aging process of the initial gel being the main factors that affect the process. Based on literature there are some different routes for the hydrothermal synthesis of SAPO-34 by Ghavipour et al. [99, 100].

1.2.4 Cocatalyst

A cocatalyst is a substance or agent that, in combination with one or more other substances, enhances the activity of a catalyst. Its use can serve various purposes, depending on the nature and composition of the substance. The focus of our discussion is the application of cocatalysts in the process of converting carbon dioxide into cyclocarbonates, which has been explored in several studies to improve reaction conditions and conversion rates. In this process, MOF is used, which contains metal ions that interact with the oxygen atoms in epoxides to activate them. This interaction results in the

weakening of the CO bond as the oxygen atom transfers electrons to the metal center. Subsequently, a nucleophilic bromine ion from the co-catalyst tetrabutylammonium bromide (TBAB) cleaves the CO bond of the coordinated epoxide. The attack of an epoxide oxygen atom on an electrophilic carbon atom in CO_2 leads to the formation of an alkyl carbonate, which undergoes intramolecular ring closure to produce cyclic carbonate. Jose et al. investigated the synthesis of cyclic carbonates catalyzed by Chromium and aluminum salphen complexes in the presence of TBAB as a cocatalyst [101]. Gupta and colleagues investigated the effectiveness of varying amounts of TBAB cocatalyst with Cu (II)-MOF (1) catalyst and demonstrated its efficacy in the process of converting carbon dioxide [101].

1.3 Research Aim and Objectives

The main objective of this research was to develop a novel SAPO-34/ZIF-8 composite as a heterogeneous catalyst for the conversion of CO_2 and epoxides into cyclic carbonates with higher added value. To fulfill the objective, the following activities were conducted:

- Synthesizing SAPO-34 catalysts.
- Fabricating SAPO-34/ZIF-8 composites with different weight percentages of ZIF-8 and SAPO-34.
- Characterizing the composites using XRD, SEM, FTIR, and BET to determine their crystallinity, morphology, functional groups and surface area, respectively.
- Investigating the effect of various process parameters such as solvent ratio, pressure, temperature, and time on the conversion of propylene oxide (PO) to propylene carbonate (PC).
- Evaluating the catalytic activity of the composite toward conversion of PO to PC and comparing it with existing research findings.
- Investigation of the catalyst reusability up to 5 runs to find out catalyst's stability and performance in a couple of tests.

1.4 Novelty of the study

The novelty of this work is the creation of dual-functional (adsorbent/catalyst) composites that combine the benefits of both substances for improved adsorption and conversion rates. In this investigation, SAPO-34 has been recognized as a cost-effective substitute for adsorption/catalysis, featuring active acidic and basic sites and a straightforward fabrication process. ZIF-8, on the other hand, is recognized for its high porosity and acidic sites. When these two catalysts are employed together, they generate favorable circumstances for the conversion of propylene oxide to propylene carbonate.

2. Materials and Methods

2.1. Materials

For the fabrication of SAPO-34 catalysts, Tetraethyl Ammonium Hydroxide Aqueous Solution (35%, TEAOH) from Alfa Aesar and Diethylamine (DEA, 99%) from Merck, were used as templates. Aluminium triisopropylate (99%) from Sigma-Aldrich, orthophosphoric acid (85%, aqueous solution) from BDH, and tetraethyl orthosilicate (TEOS, 99%) from Sigma-Aldrich served as the sources of Al, P, and Si, respectively. Commercial companies such as Alfa Aesar and Fisher Scientific supplied the materials and reagents for ZIF-8 production. The synthesis of ZIF-8 involved the use of 2-methylimidazol (2-MIM) (97.0%) from Alfa Aesar, acetone (99.5%) from Fisher Scientific, and zinc nitrate hexahydrate (99.0%) from Alfa Aesar. All chemicals were used as received without any further purification.

2.2 Nanostructured Catalyst Preparation and Procedure

2.2.1. Preparation of the SAPO-34

SAPO-34 was synthesized using the hydrothermal method [102]. Initially, triisopropylate aluminium and TEAOH were dissolved in deionized water and allowed to dissolve for 90 minutes. The solution

was then gradually diluted with phosphoric acid while stirring for 30 minutes. Subsequently, the Si precursor was added to the solution and stirred for an additional 30 minutes. The final step involved the addition of DEA to the solution, which was stirred for 24 hours. The resulting mixture was transferred to a Teflon-lined stainless autoclave reactor and subjected to hydrothermal treatment at 200°C for 48 hours. The resulting material was then centrifuged, washed with distilled water three times, and dried overnight at 110 °C. Finally, the nanostructured sample underwent calcination at 550 °C for 12 hours to remove the templates.

2.2.2 Sy*nthesis of ZIF-8*

ZIF-8 nanocrystals were synthesized using the methodology outlined in previous studies [103]. The standard procedure involved adding zinc nitrate hexahydrate and 2-MIM precursors separately into different beakers. The mixture was then agitated in 30 mL of acetone for 10 minutes at an 8:1 molar ratio. Subsequently, the solutions were combined and stirred for two hours. The resulting mixture was washed three times with acetone and the obtained product was dried overnight at 85 ℃ in a vacuum oven.

2.2.3 Preparation of SAPO-34/ZIF-8 composite

The composite materials were prepared as illustrated in Figure 1 [104]. Initially, the synthesized SAPO-34 was dissolved in acetone for 15 minutes and subsequently dispersed in a bath ultrasound for 0.5 hours. After that, 2-MIM and zinc nitrate hexahydrate were added in an 8:1 ratio, and the solution was mixed for 2 hours. The resulting product was washed three times with acetone and dried overnight at 85°C in a vacuum oven.

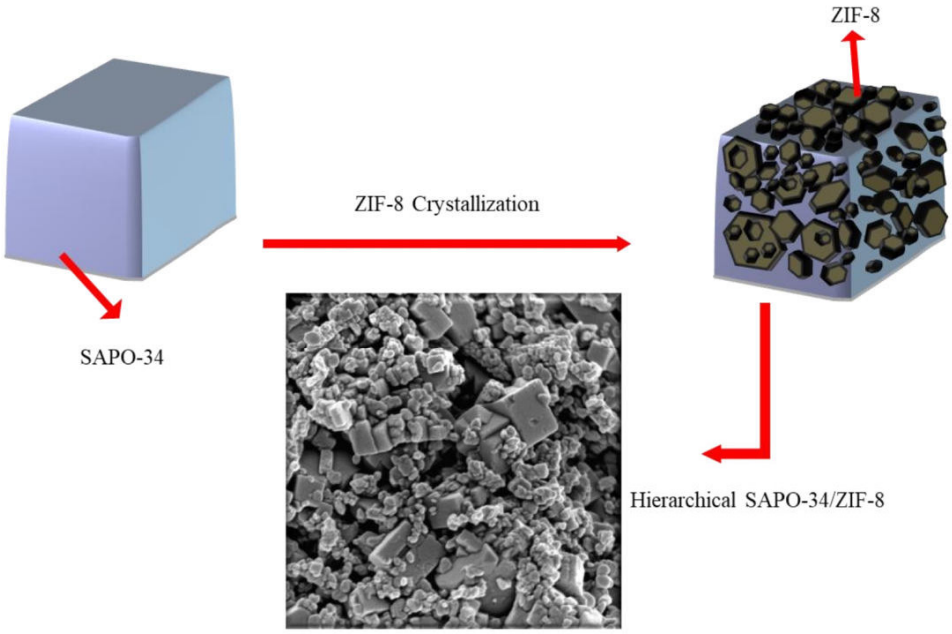

Figure 1. Heterogeneous crystallization of ZIF-8 over the SAPO-34.

Table 2 presents the fabrication of SAPO-34 and ZIF-8 using the epitaxial growth technique, with varying weight percentages.

Table 2. Chemical compositions used for synthesising of composites.

ZIF-8 (wt.%)	SAPO-34 (wt.%)	Composite
100	0	ZIF-8
25	75	S/Z25
50	50	S/Z50
75	25	S/Z75
0	100	SAPO-34

2.2.4 Characterization of the Nanostructured Catalyst

The composite phases were determined through X-ray diffraction (XRD) analysis using a Miniflex 600 6G (Rigaku, Japan) diffractometer. CuKα radiation (λ=1.5406 Å) was employed at 40 kV and 15 mA, covering a 2θ range of 5° to 60°. Surface area, pore volume, and pore diameter of the composites

were measured using the Brunauer-Emmett-Teller (BET) technique with a Quantachrome Instruments (USA) instrument. The identification of functional groups was conducted in the samples using Fourier-transform infrared spectroscopy (FTIR) with a Bruker ALPHA II spectrometer. The morphology of the synthesized composites was examined using scanning electron microscopy (SEM) with a CHTP Helios 650 instrument.

2.2.5 *Catalyst Performance Test*

Catalyst testing on the synthesized composites was conducted in a 300 mL stainless-steel reactor, in accordance with the experimental design. The reactor was heated to the desired temperature, and the necessary pressure for each test was achieved by utilizing a CO_2 gas cylinder equipped with a high-pressure regulator. To optimize heat transfer and minimize energy loss, an oil bath was employed for all reactions. The reaction temperature was 5°C lower than the temperature on the hot plate due to the presence of the oil bath. After submerging the reactor in the oil bath for 30 minutes, the temperature reached a steady state and remained constant throughout the reaction process. Figure 2 illustrates the experimental setup used in this study, and the reaction time was recorded once the oil bath temperature reached a stable state. In other words, the autoclave was then pressurized with CO_2 to the desired level and heated to a specific temperature. Subsequently, the reaction was initiated by stirring at a speed of 300 rpm. Once the reaction was complete, the reactor was cooled to room temperature and any remaining unreacted CO_2 was gradually released. The catalytic product conversion was evaluated using ^{1}H-NMR spectroscopy through the integration of proton A (clearly resolved signal) from the epoxide, and proton A from the carbonate, according to the given Eq. 1 [105].

$$(\%)Conversion = \frac{I\,HA\,(carbonate)}{I\,HA(carbonate)+I\,HA(epoxide)} * 100 \qquad \text{(Eq. 1)}$$

Where I H_A (carbonate) and I H_A (epoxides) are the integration values of proton A form the carbonate and epoxide respectively.

To improve the conversion value of PO to PC by catalysts, it was necessary to evaluate several parameters. Therefore, further studies conducted on the most appropriate composite in terms of the most suitable conversion. The analysis was performed to extract several data sets using variables specified within the software, including temperature, pressure, and time.

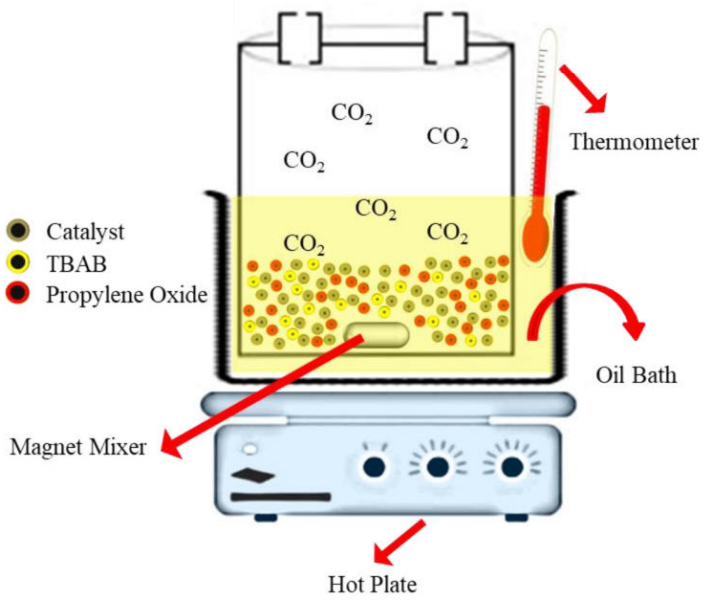

Figure 2. Experimental setup for catalytic conversion of CO_2

3. Results and Discussions

3.1 Nanostructured Catalyst Characterization

3.1.1 XRD Analysis

Figure 3 illustrates a comparison of the powder X-ray diffraction (XRD) patterns among the samples of SAPO-34, ZIF-8, S/Z75, S/Z50, and S/Z25, alongside the corresponding reference patterns obtained from JCPDS numbers. The XRD patterns of the synthesized S/Z composites, pristine ZIF-8, and SAPO-34 can be attributed to the JCPDS File No. "00-062-1030" and "01-087-1527," respectively [106, 107].

The XRD pattern of the composites exhibits similarities to both SAPO-34 and ZIF-8, indicating the absence of impurities. Identified diffraction peaks for ZIF-8 were observed at 2θ values of 7.34, 10.39, 12.74, 18.05, and 26.7 °, corresponding to the crystallographic planes (110), (200), (211), (222), and (431). SAPO-34 exhibited diffraction peaks at 2θ values of 9.47, 12.85, 15.98, 17.74, and 20.56 °, associated with the crystallographic planes (1 0 1), (1 1 0), (0 2 1), (0 0 3), and (1 2 -1), respectively. The analysis of the XRD patterns of composites demonstrate that when the ZIF-8 loading is increased from 25 to 75 wt.%, there is a reduction in the intensity of characteristic peaks related to SAPO-34. These results indicate that ZIF-8 is present as a coating on the surface of SAPO-34. Importantly, the intensities and positions of the XRD peaks for ZIF-8, SAPO-34, and the synthesized composites confirm the preservation of structural stability in both ZIF-8 and SAPO-34, indicating the successful synthesis of all composites with various weight percentages.

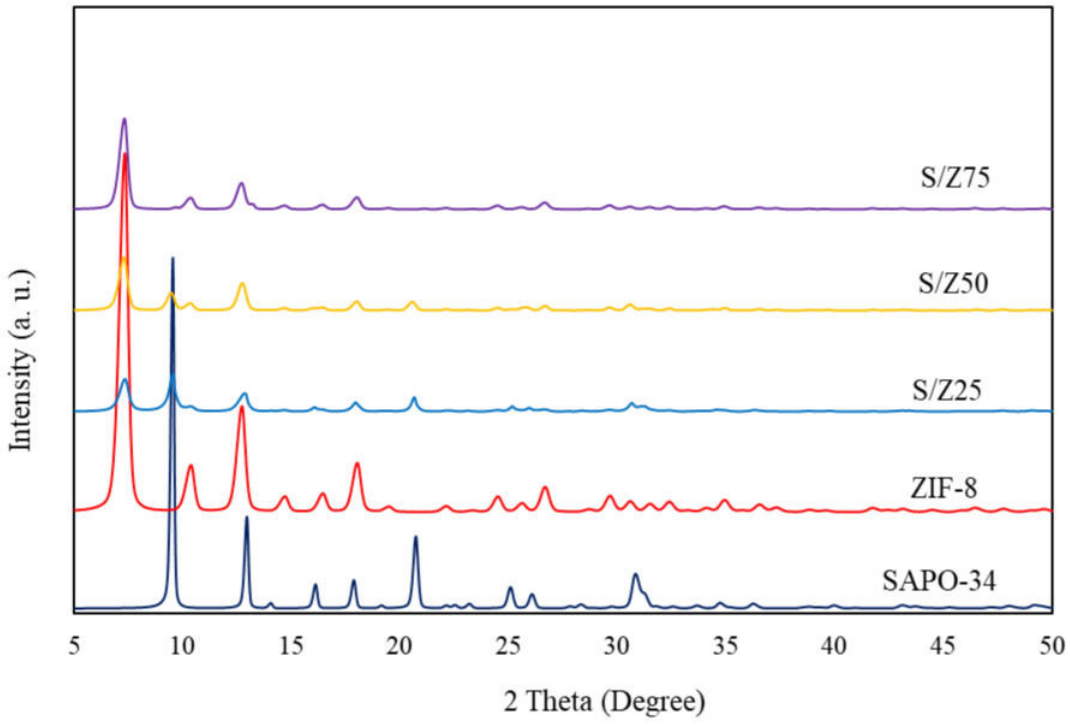

Figure 3. XRD patterns of synthesized catalysts: SAPO-34, ZIF-8, S/Z75, S/Z50, and S/Z25.

3.1.2 SEM Analysis

The SEM images (Figure 4) reveal that pristine ZIF-8 nanocrystals with a consistent particle size of approximately 50 nm which confirms a notable effect of acetone on reducing the particle size of ZIF-8 [108]. The particle size distribution of ZIF-8 ranges from 28 to 76 nm, while conventional SAPO-34 exhibits a particle size of around 215 nm (Figure A 1).

Moreover, SEM images offer compelling visual confirmation that the ZIF-8 particles were synthesized in close proximity to the SAPO-34 particles, enveloping them in the process. This observation strongly indicates a phenomenon of heterogeneous nucleation and growth, wherein the ZIF-8 structure developed atop the SAPO-34 particles, resulting in the successful synthesis of these composite materials. Moreover, the SEM images further substantiate the distinctive morphologies of the particles, showcasing SAPO-34's characteristic cubic shape and ZIF-8's hexagonal shape. Consequently, these SEM images offer added validation for the preservation of the desired shapes within SAPO-34 and ZIF-8, providing robust confirmation of the successful synthesis and formation of the intended composites.

As the primary objective of this study revolves around assessing the extent of CO_2 conversion using the synthesized catalysts, it becomes apparent that an increase in the agglomeration of ZIF-8 particles on SAPO-34 leads to a higher CO_2 adsorption capacity. However, this phenomenon has a contrasting effect as it simultaneously results in the coverage of functional groups within SAPO-34, subsequently diminishing the overall conversion efficiency which subsequent experimental investigations, including BET analyses and conversion studies, substantiate and validate this intricate relationship.

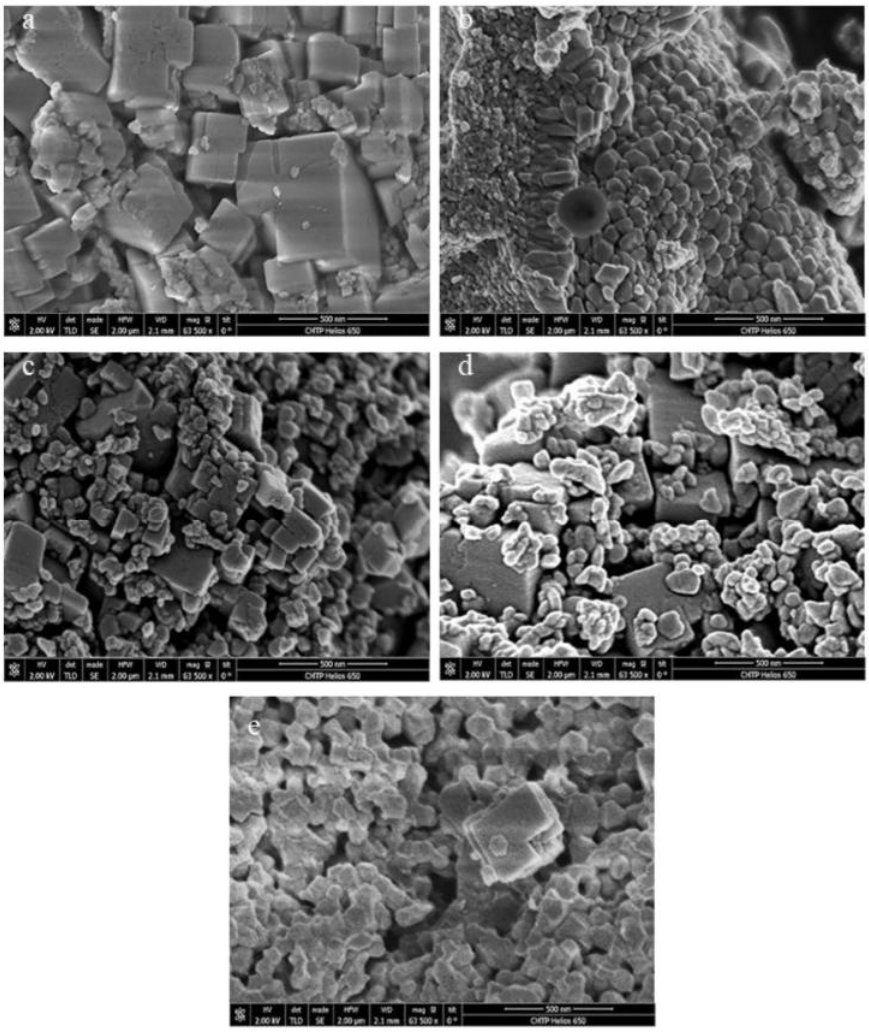

Figure 4. SEM images of (a) SAPO-34, (b) ZIF-8, (c) S/Z25, (d) S/Z50, and (e) S/Z75 (scale= 500 nm).

3.1.3 FTIR Analysis

FTIR was applied to determine the functional groups of synthesized compounds and presented in Figure 5. The characteristics bands for ZIF-8 and SAPO-34 were consistent with those previously reported in the literature [109, 110]. The majority of the absorption bands of synthesized ZIF-8 can be attributed to the imidazole moiety. The band peaks between 1310-1425 cm^{-1} are attributed to entire ring stretching whereas an aromatic C-N stretching signal was found at 1146 cm^{-1} [110]. The characteristic peaks at 995 cm^{-1} and 759 cm^{-1} could be corresponded to C-N bending vibrations and

C-H bending modes [111]. The peaks at 694 cm^{-1} represents out-of-plane bending for imidazole ring [112].There was a strong stretching vibration band observed at 426 cm^{-1} for the Zn-N indicating the chemical interaction of zinc ions with nitrogen atoms of the methylimidazole groups towards the creation of imidazolate [111, 113]. Furthermore, the results obtained from the FTIR data analysis of synthesised SAPO-34 indicate a strong agreement between the characteristic vibration peaks of its functional group and those reported in the literature [114].

The following vibrational frequencies can be attributed to specific molecular motions: 730 cm^{-1} corresponds to the symmetric stretching of the O–P–O bond, 640 cm^{-1} arises from the bending motion of a double 6-ring structure, 575 cm^{-1}, 530 cm^{-1}, and 480 cm^{-1} are associated with the bending of PO_4, AlO_4, and SiO_4, respectively [115]. The correct formation of composites S/Z75, S/Z50, and S/Z25 can be confirmed by matching the FTIR diagrams of samples SAPO-34 and ZIF-8. Therefore, it is evident that both SAPO-34 and ZIF-8 offer a wide range available active sites as a support and active phase, respectively, as confirmed by SEM analysis.

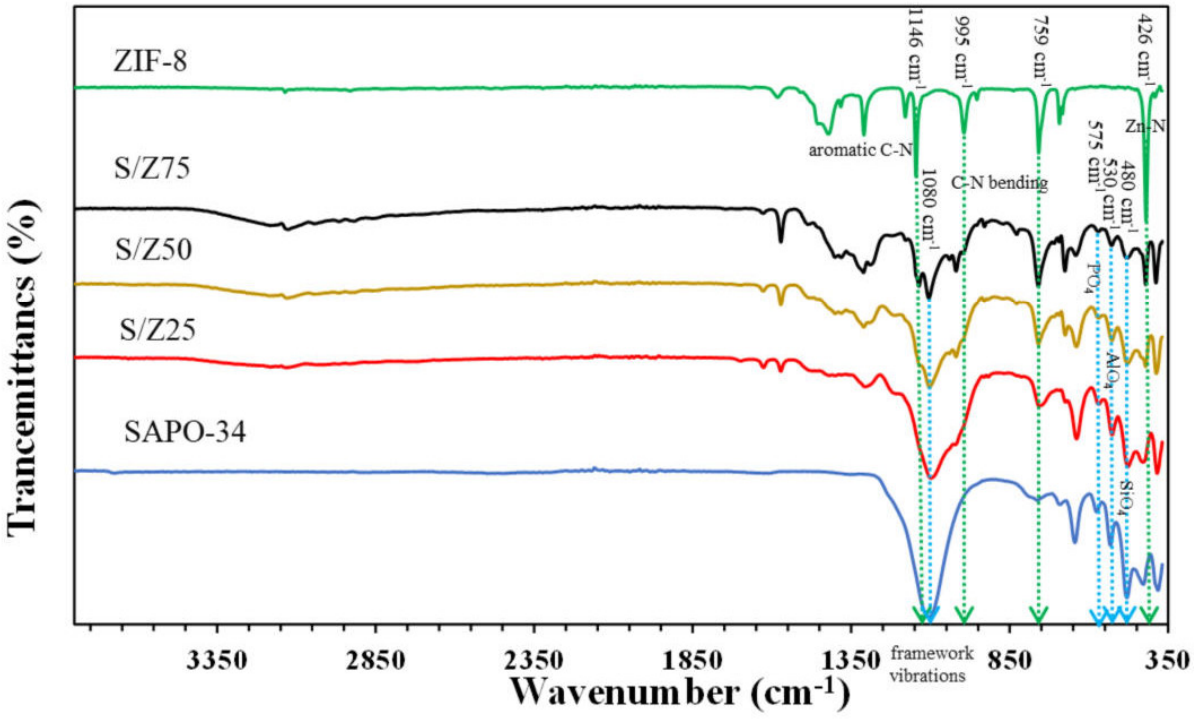

Figure 5. FTIR spectra of SAPO-34, ZIF-8, S/Z25, S/Z50, and S/Z75.

3.1.4 BET-BJH Analysis

BET-BJH analysis was applied on SAPO-34, ZIF-8, S/Z25, S/Z50, and S/Z75 to assess the impact of composite synthesis on their surface area and porosity. The surface areas, pore volume and pore size of the pristine catalysts and composites based on BET adsorption and desorption of N_2 are shown in Table 3. It is obvious that the creation of the SAPO-34 and ZIF-8 composites decrease the BET surface area compared to pure SAPO-34 (550 m^2/g). This likely occurred because of the penetration of ZIF-8 particles into the pores of SAPO-34. Taking into this matter the pore volume values for ZIF-8 (0.51 cm^3/g) and SAPO-34 (0.21 cm3/g), it becomes evident that the volumes of the original catalysts have larger micropore volume values than that of the composites. Also, it is evident that S/Z25 has a larger pore size than the other synthesized pristine catalysts and composites. Larger pore (mesopore) size enhances mass transfer which allows larger molecules to diffuse more freely which the catalysts. Therefore, they facilitate the movement of reactants and products which causes the long catalyst life. Therefore, S/Z25 is expected to have higher PO conversion value due to its mesoporous structure.

Table 3. BET Surface Area of ZIF-8, SAPO-34, and optimized composite (S/Z25).

Samples	**ZIF-8**	**SAPO-34**	**S/Z25**	**S/Z50**	**S/Z75**
BET Surface Area (m^2/g)	1200	550	50	85	188
Total Micro Pore Volume (cm^3/g)	0.51	0.21	0.1	0.08	0.07
Total BJH Pore Volume (cm^3/g)	0.18	0.34	0.17	0.09	0.05
Average BJH Pore Diameter (nm)	11.3	16.6	20	18.5	12.7

3.2 CO_2 Cycloaddition of PO Over Composites

3.2.1 Experimental Design and effect of temperature, pressure, and time on Conversion

The optimal combination of pressure, temperature, and time towards CO_2 cycloaddition of PO was explored. A conversion value of 90% was successfully achieved within the composite containing 75 wt.% of SAPO-34 and 25 wt.% of ZIF-8 (S/Z25) which is in good agreement with SEM and BET-BJH results. In order to identify the optimal catalyst among the synthesized options for future experimental designs, initial tests were conducted on all catalysts under identical operational conditions, with the presence of a co-catalyst, Tetrabutylammonium Bromide (TBAB). Table 4 table effectively demonstrates the conversion values, which were calculated using the extracted data from the ^{1}H NMR analysis. The tabulated information was enhanced by incorporating the results from ^{1}H NMR analysis Figures A2, A3, A4, A5, A6, and A7 illustrate the procedure for calculating PO conversion to PO, as well as the ^{1}H NMR outcomes for PO, PC, the pristine catalysts (specifically ZIF-8 and SAPO-34), and the optimized composite. Using the surface response method, an experimental design was carried out for the PO cycloaddition reaction by S/Z25. This design incorporated the independent variables utilized in Table A 1, considering the findings related to the optimum conversion value from Table 4. The amount of catalyst, TBAB and PO which were used in the reaction were 0.4, 0.62 g, and 59.16 mL respectively. Besides, the mean conversion values for different designed operational variables were revealed in Figure 6. At the evaluated range of temperature, time, and pressure in this study, the following observations were made:

Table 4. PO conversion evaluation by synthesized catalysts [a]

Catalyst	Conversion (%)[a]
SAPO-34	78.85
ZIF-8	75.75
S/Z75	81.2
S/Z50	80
S/Z25	90

[a] Conversion was determined by ^{1}H NMR.

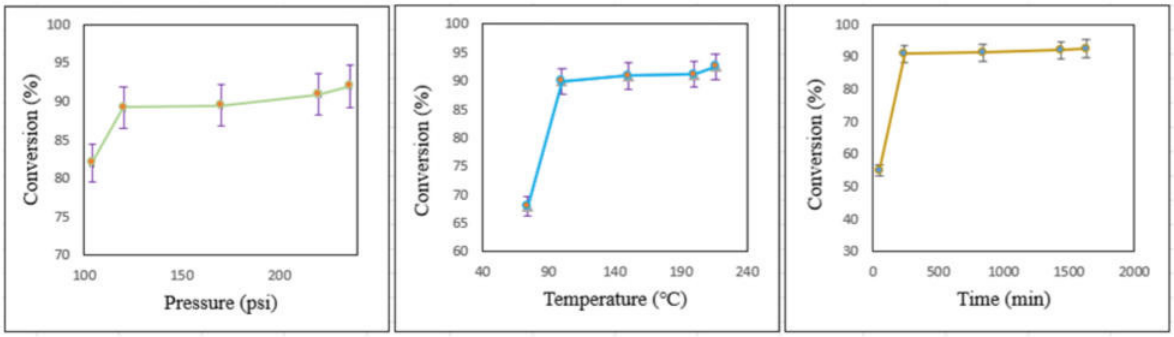

Figure 6. The mean effect plots for the mean CO_2 conversion [a] percentage in contact pressure (psi), temperature (°C) and time (min) using surface response method via 0.4 g catalyst, 0.62 mmol TBAB, and 59.16 mmol PO.

[a] The middle data points were obtained from five replicates, while the initial and final data points were derived from three replicates.

3.2.2 Catalytic Performance at Various Amounts of Catalyst

The experimental conditions, characterized by high catalytic activity as outlined in the preceding section, were selected for further testing with varying amounts of catalyst, as illustrated in Scheme 1. This investigation revealed that the optimal catalyst quantity for this reaction was 0.4 g. Importantly, augmenting the catalyst amount beyond this value showed no substantial impact on the conversion rate. Conversely, decreasing the catalyst amount from 0.5 g to 0.1 g led to a reduction in the CO_2

conversion rate from 93% to 70.92%. The CO_2 conversion percentages corresponding to varying catalyst amounts are visually depicted in Figure 7, derived from the ^{1}HNMR data (Figure A 6).

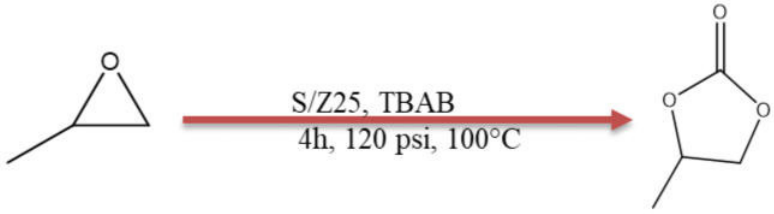

Scheme 1. CO_2 conversion with epoxides using synthesised catalysts under optimized conditions.

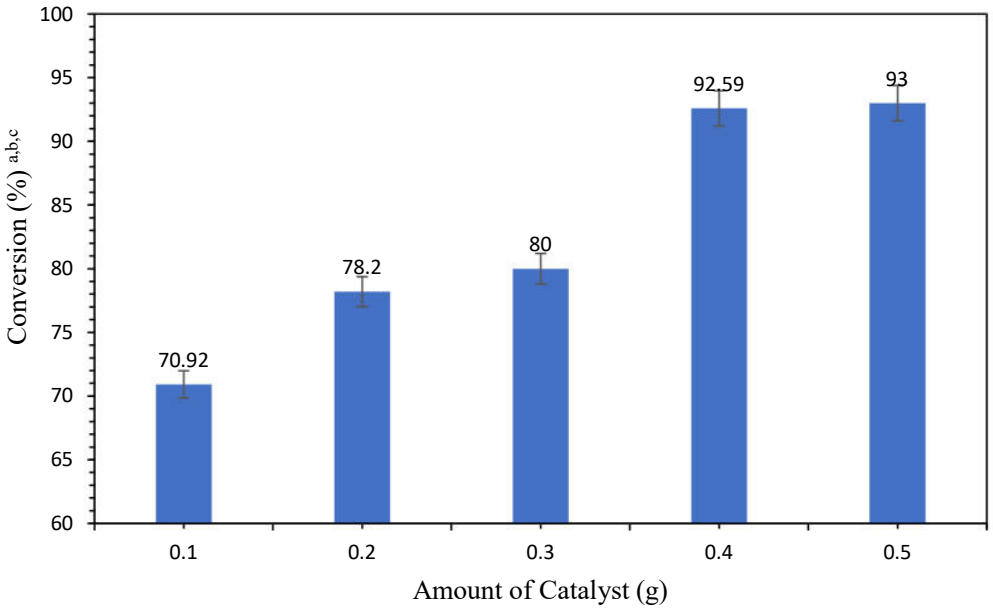

[a] Reaction conditions: 0.62 mmol TBAB, 59.16 mmol PO, 120 psi, 100 °C, 240 min

[b] Conversion was determined by ^{1}H NMR

[c] Three replicates for each point

Figure 7. Loading of different amount of S/Z25 for CO_2 cycloaddition reaction.

3.2.3 Reusability Test of the Synthesized Composite

To assess the catalyst's lifetime and compare the outcomes of PO conversion, reusability testing was conducted for five cycles. Figure 8 displays the positive results obtained from the catalyst's reusability. After each reaction, the catalysts were subjected to centrifugation at 12000 rpm and 4 °C

to separate the liquid and solid phases. Prior to centrifugation, the catalyst was rinsed three times with methanol under the same conditions. Subsequently, a drying process at 65°C was carried out overnight for each reaction. The conversion values of the fresh catalyst and the catalyst reused for three cycles were found to be the same. However, in the 4th and 5th runs, a slight deviation in the conversion value was observed. It's important to highlight that each data point was replicated three times. This repetition helps ensure the reliability and consistency of the measurements or observations.

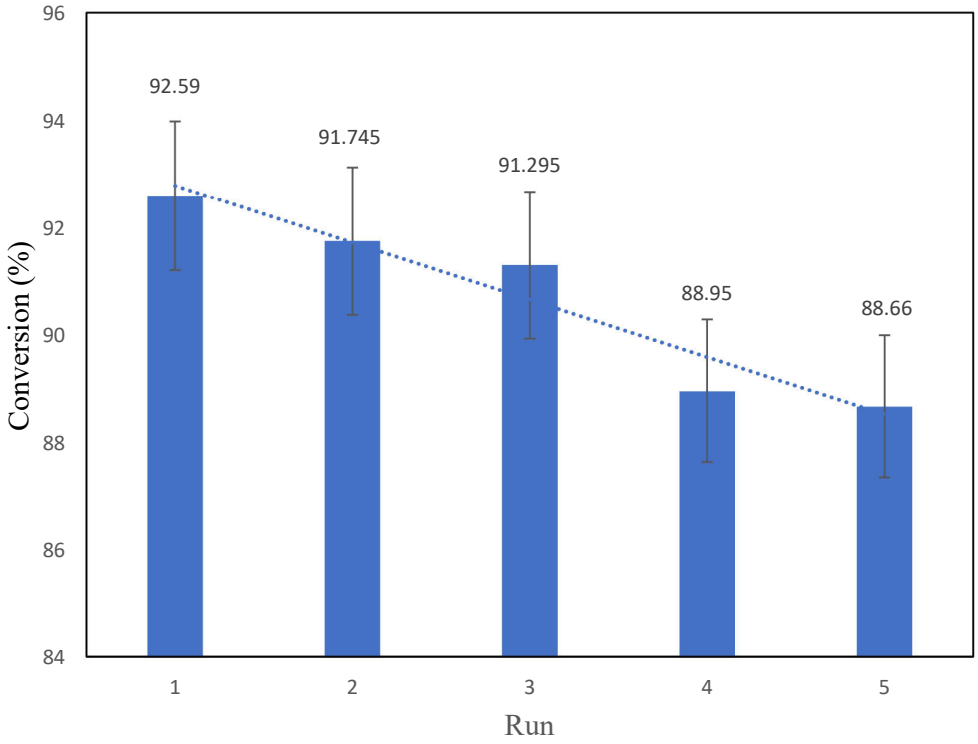

Figure 8. Reusability test; S/Z25 (0.4 g), TBAB (0.62 mmol), 59.16 mmol PO, 100 °C, 240 min and 120 psi.

3.2.4 Catalyst Influence on PO Conversion: Comparative Analysis of Operating Conditions

The catalytic reactions of epoxide with CO_2 have already been performed with different catalysts. Table 5 provides a comparison of PO conversion rates obtained from various catalysts and operating

conditions. The table incorporates data from both existing literature and our current study. The available data indicates the potential for achieving a higher conversion rate using ZIF-95 [113]. This particular reaction involved utilizing 18.6 mmol of PO over a 2-hour period, operating at 174 psi and 80°C. Similarly, the reaction was conducted using ZIF-23 as a catalyst, resulting in the conversion of 42.87 mmol of PO to cyclic carbonate within 6 hours, employing the same pressure and temperature parameters [116, 117]. Under comparable operational circumstances, the present work (S/Z25) exhibited an excellent capacity for conversion compared to alternative catalysts. This composite was able to transform 92.59% of 57.16 mmol of PO into cyclic carbonate. This conversion rate is much greater than that achieved with the original pristine MOFs which have been used for PO conversion in this table.

Table 5. The comparison for PO conversion using different catalysts and operating conditions.

Entry	Name	Cat. amount	PO (mmol)	Time (h)	P CO_2 (psi)	Temp. (°C)	Co Cat. (mmol)	PO Con. (%)	Ref.
1	ZIF-23	0.8 mmol	42.87	6	174	80	0.8	55.6	[117]
2	MIL/K-OH	0.85 mmol	24	24	174	50	0.85	77	[116]
3	NH_2-MIL-53(Al)	0.85 mmol	24	5	116	80	0.85	65	[116]
4	ZIF-95[a]	0.4 mmol	18.6	2	174	80	0.4	91	[111]
5	ZIF-78	0.05 g	20	15	142.2	150	N/A	88	[113]
6	ZIF-8	0.85 mmol	24	24	116	80	0.85	67.9	[118]
7	SAPO-34	0.8 mmol	71.45	5	150	150	0.54	78.85	This work
8	ZIF-8	1.53 mmol	71.45	5	150	150	0.54	75.75	This work
9	S/Z75	3.5 mg	71.45	5	150	150	0.54	81.2	This work
10	S/Z50	3.5 mg	71.45	5	150	150	0.54	80	This work
11	S/Z25	3.5 mg	71.45	5	150	150	0.54	90	This work
12	S/Z25	4 mg	59.16	4	120	100	0.62	92.59	This work

3.2.5 Proposed mechanism of reaction for CO_2 conversion using synthesized composite

Figure 9 explores the proposed mechanism for producing polycarbonate PC using S/Z25 catalyst. Using the dual-functional catalytic system, consisting of a Lewis acidic site (S/Z25) and a nucleophilic co-catalyst (TBAB), plays a pivotal role in catalytic activity [119]. We propose a

potential mechanism for the cycloaddition reaction of CO_2 with PO. In this mechanism, the synthesized composite acts as a dual-functional binary catalyst system, with metals in the composite acting as unsaturated Lewis acids to activate the epoxide ring. The nucleophilic attack of carboxylate groups from SAPO-34 (basic sites) and Br- (generated from TBAB) opens the epoxide ring, forming a zwitterion. In the final stage, the metal carbonate species moves through, eliminating the bromide ion. The active catalyst is renewed simultaneously as the cyclic carbonate is removed from the metal core. The mechanism highlights the independent dual functionality of SAPO-34 and ZIF-8 as adsorbent/catalysts. However, when ZIF-8 is the active phase and SAPO-34 serves as the supporting adsorbent catalyst, CO_2 adsorption, the initial step in the conversion process, significantly improves. Furthermore, both materials act as catalysts, synergistically utilizing their functional groups to fixate CO_2, resulting in a higher conversion rate. This advancement positions ZIF-8 for potential entry into the industrial arena showcasing increased economic value in terms of catalytic activity and stability.

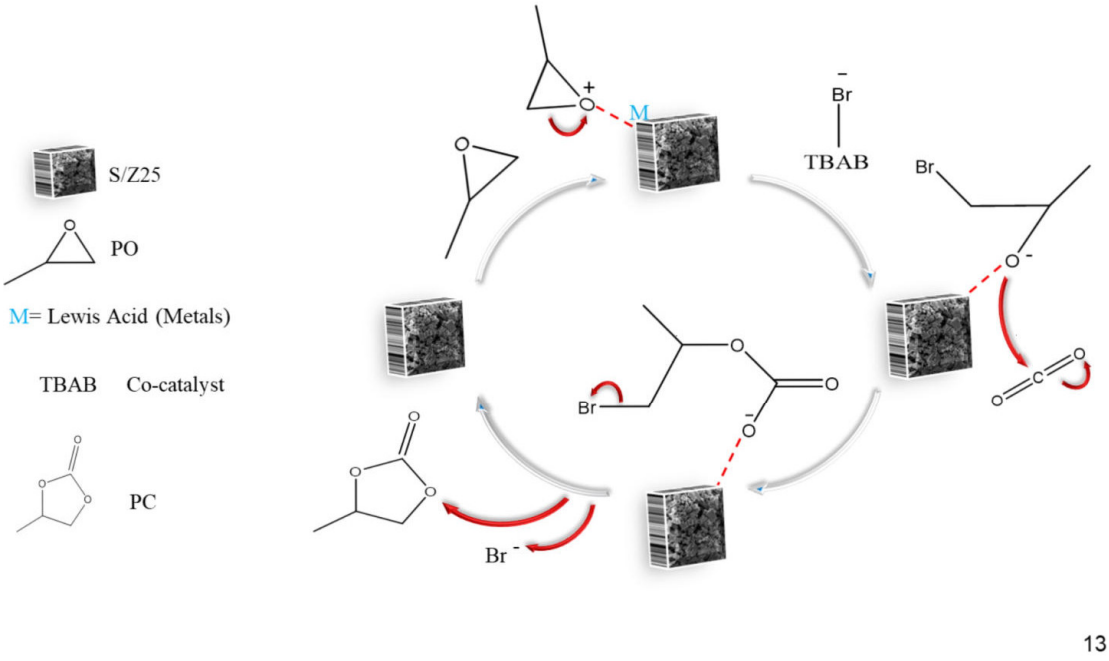

13

Figure 9. Plausible mechanism for the conversion of PO to PC using S/Z25 composite.

4 Conclusions

This research successfully utilized ZIF-8 and SAPO-34 to fabricate a novel composite. The epitaxial growth method was employed to prepare a SAPO-34/ZIF-8. The synthesized catalysts underwent characterization using XRD, SEM, FTIR, and BET techniques. Among the composites, SAPO-34/ZIF-8 75:25 wt.% exhibited significant suitability as a catalyst for propylene carbonate synthesis. The formation of SAPO-34/ZIF-8 composites resulted in increased conversion values, acid and active sites, and extended catalyst lifetime. An experimental design approach was employed to optimize the operational factors. Remarkably, a conversion rate of 92.59% was achieved at a pressure of 120 psi, temperature of 100 °C, and a reaction time of 240 minutes. Furthermore, the catalytic activity of the synthesized composite was tested over 5 cycles under the same conditions, demonstrating its long-lasting performance.

5 Future Study

Further investigation of the novel adsorbent/catalyst can be in the following areas:

- The examination of different epoxides, such as styrene oxide and ethylene oxide, at various quantities can be employed to gauge product conversion rates and byproduct formation.
- Different synthesis methods can be conducted in future research such as: doping strategies, and preparation processes.
- Using other adsorbent/catalysts as a support instead of SAPO-34 in the different and same wt.% ratio to evaluate catalytic activity and stability in different operational conditions.
- Conducting reaction on the different epoxides in a continuous reactor at different temperatures and low pressure.
- Evaluation of reaction in presence of various gas flow to examine the selectivity of adsorbent/catalysts in terms of adsorption and catalytic activity.
- Evaluation of effect of different amount of humidity on conversion value and catalytic activity

Appendix

Table A 1. Independent variables to determine the optimized condition using the Surface Response method.

Factors	Min	Max
Pressure (psi)	120	220
Tempreture (°C)	100	200
Time (min)	240	1440

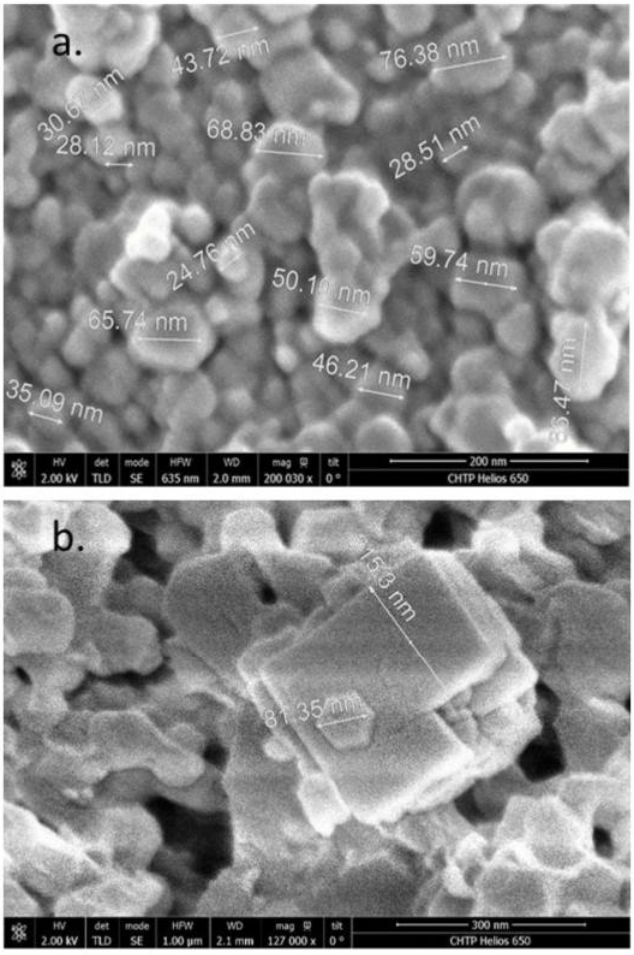

Figure A 1. a: Particle size distribution of ZIF-8; Average particle size: 48 nm; b: Particle size of SAPO-34

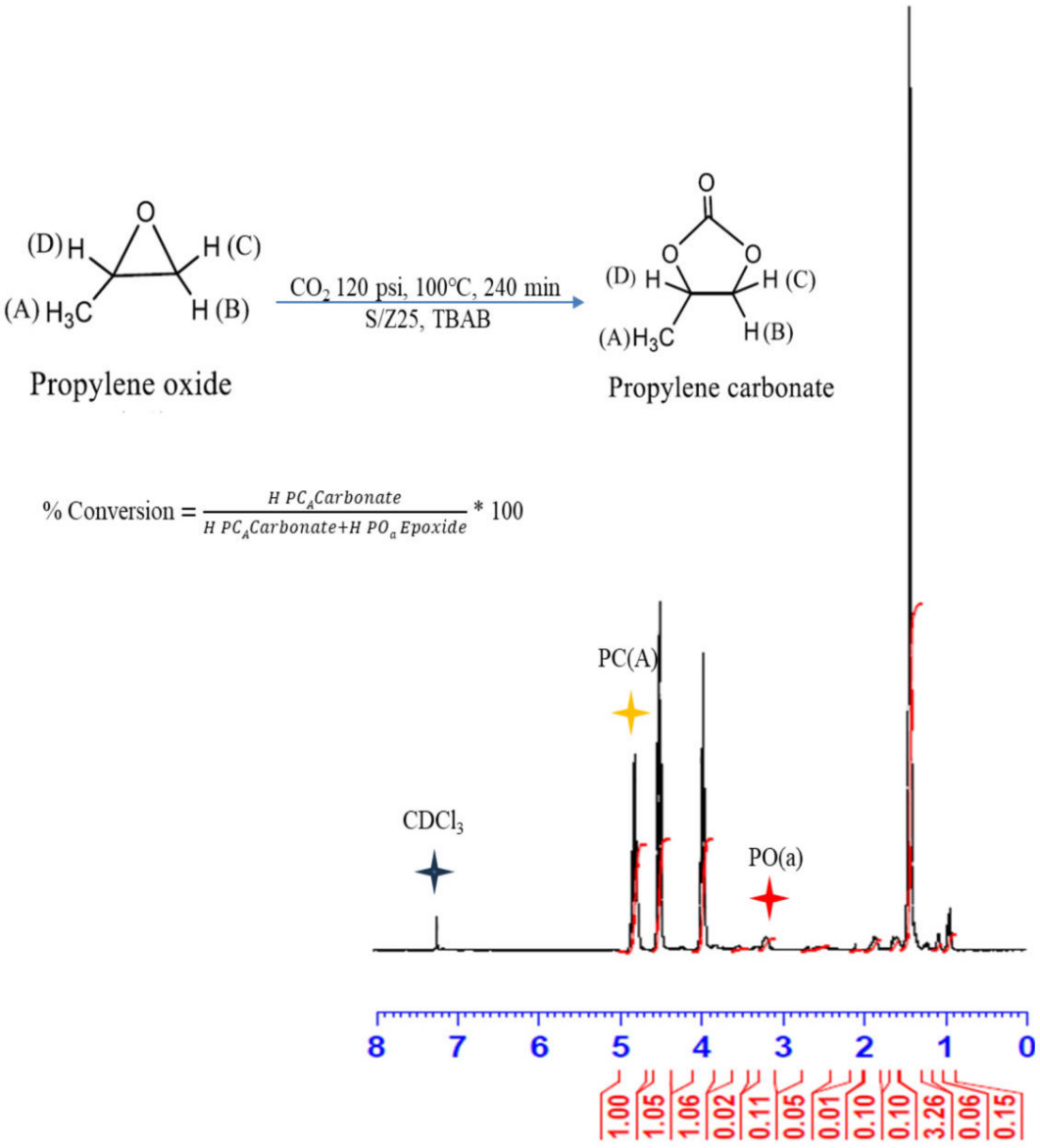

Figure A 2 . ^{1}H NMR of producing Propylene Carbonate during CO_2 conversion using Propylene epoxide

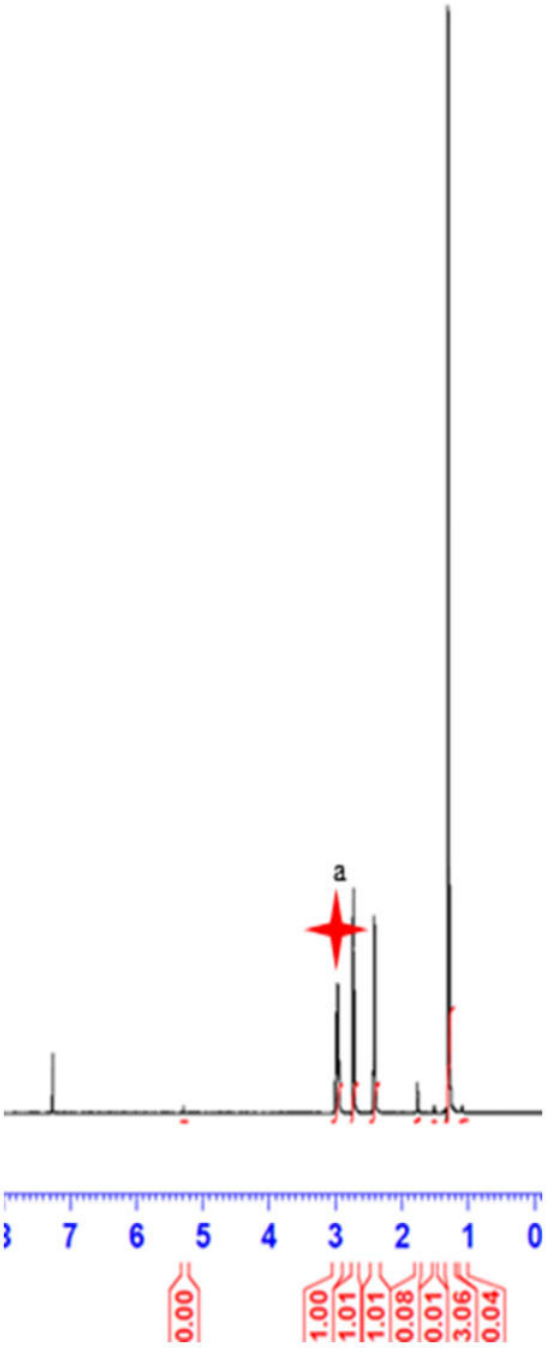

Figure A 3. ^{1}H NMR Analysis of pure PO

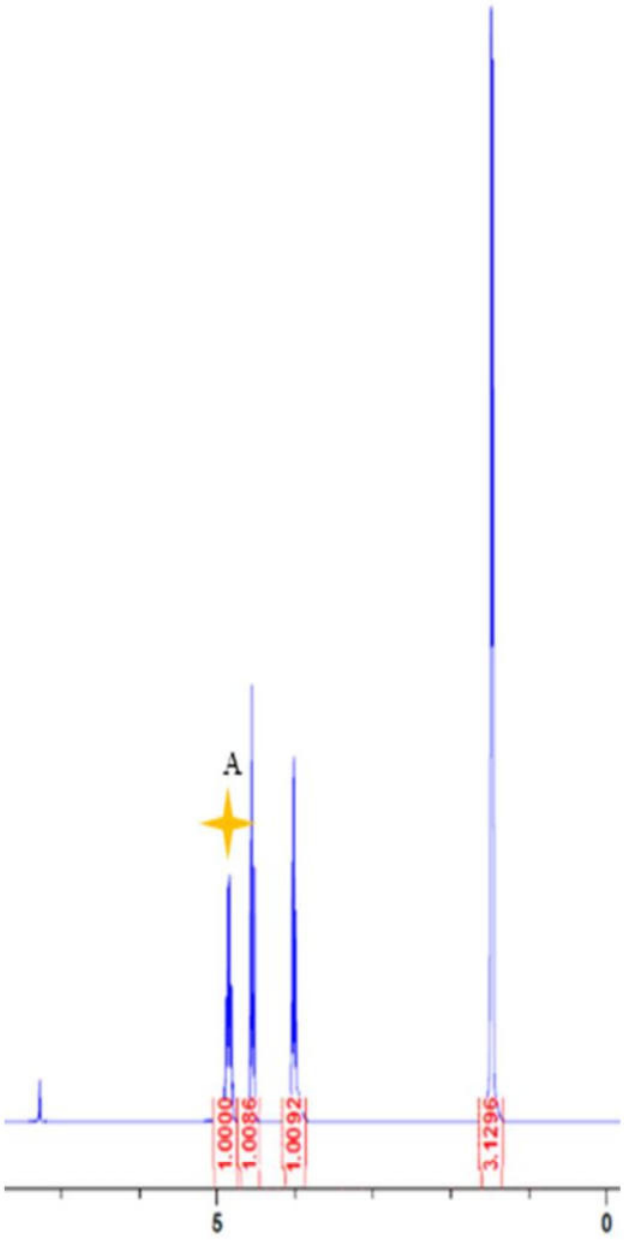

Figure A 4. ^{1}H NMR Analysis of pure PC

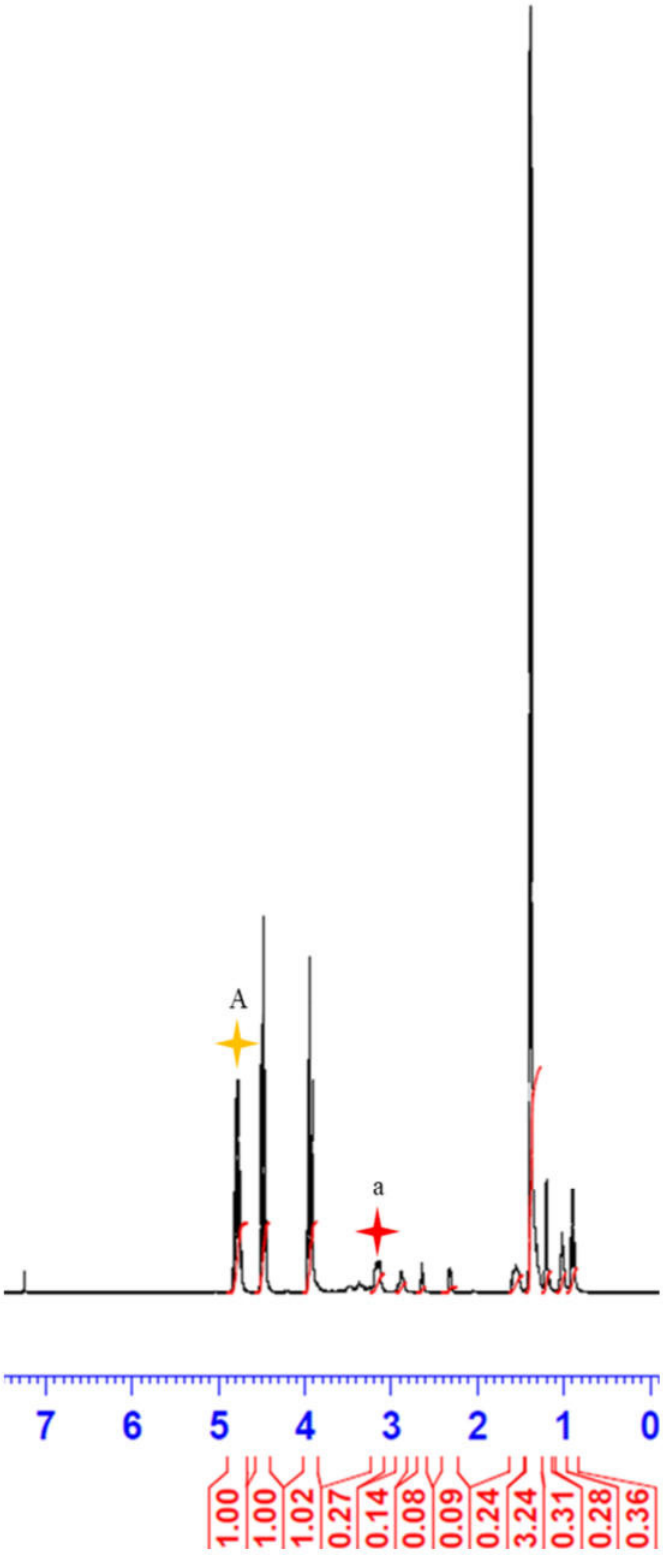

Figure A 5. ^{1}H NMR Analysis: PO conversion to PC via SAPO-34, A: PC (A) and a: PO (a)

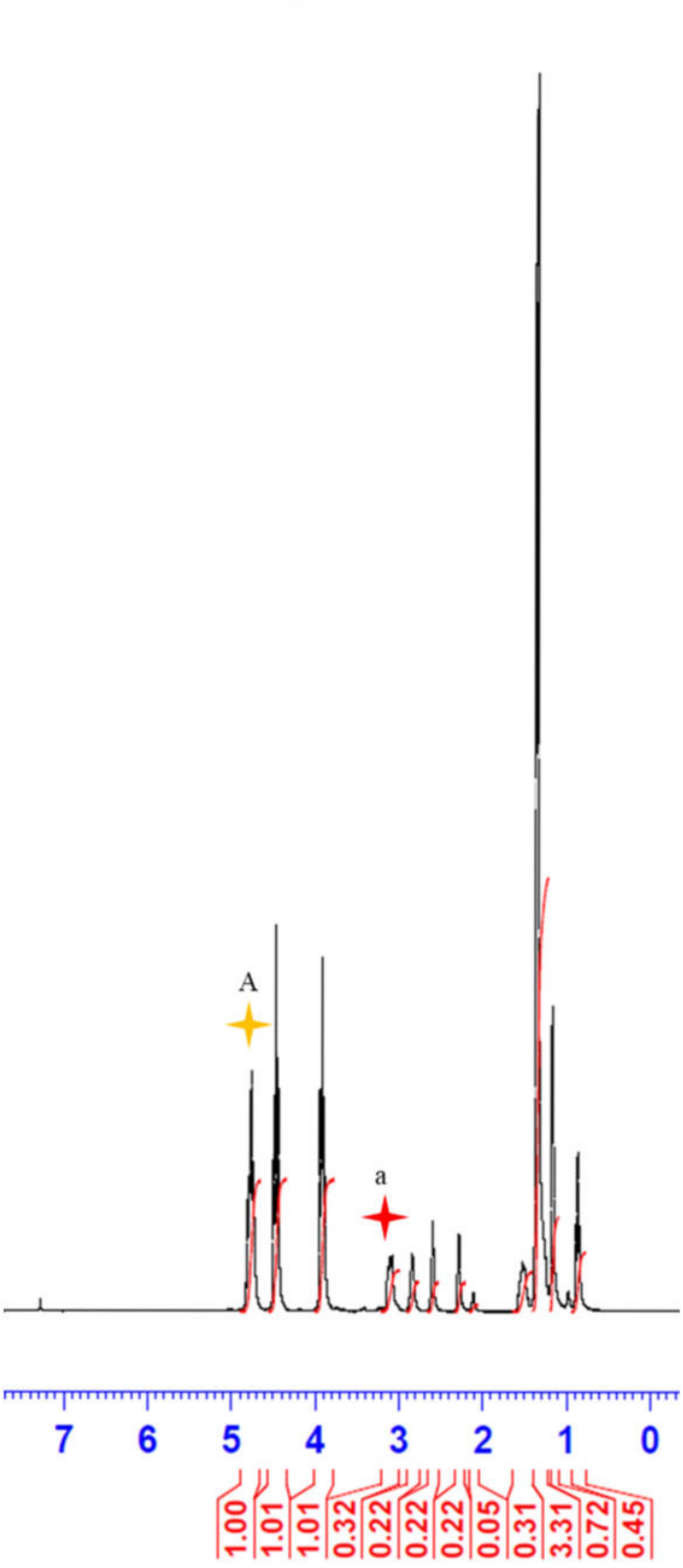

Figure A 6. ^{1}H NMR Analysis: PO conversion to PC via ZIF-8; A: PC (A) and a: PO (a)

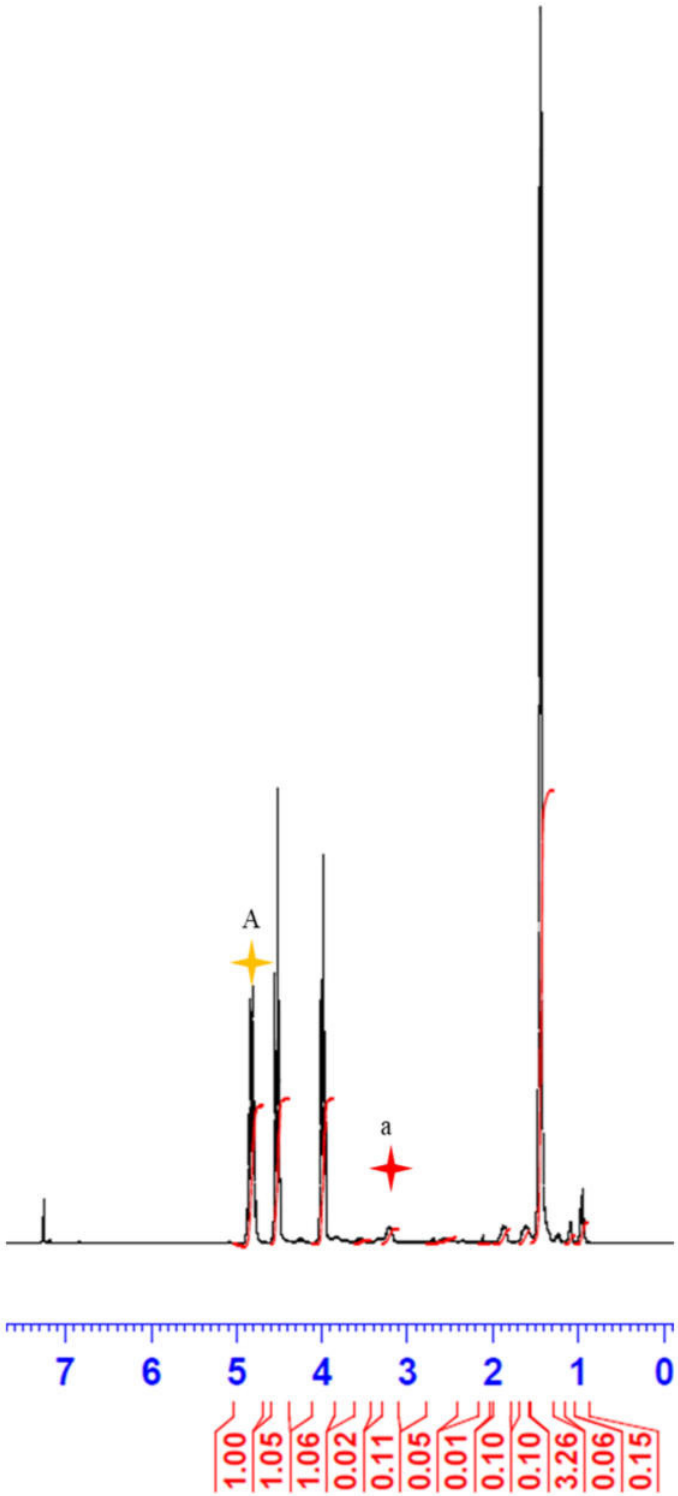

Figure A 7. ^{1}H NMR Analysis: Influence of S/Z25 composite creation on the conversion of PO to PC; A: PC (A) and a: PO (a)

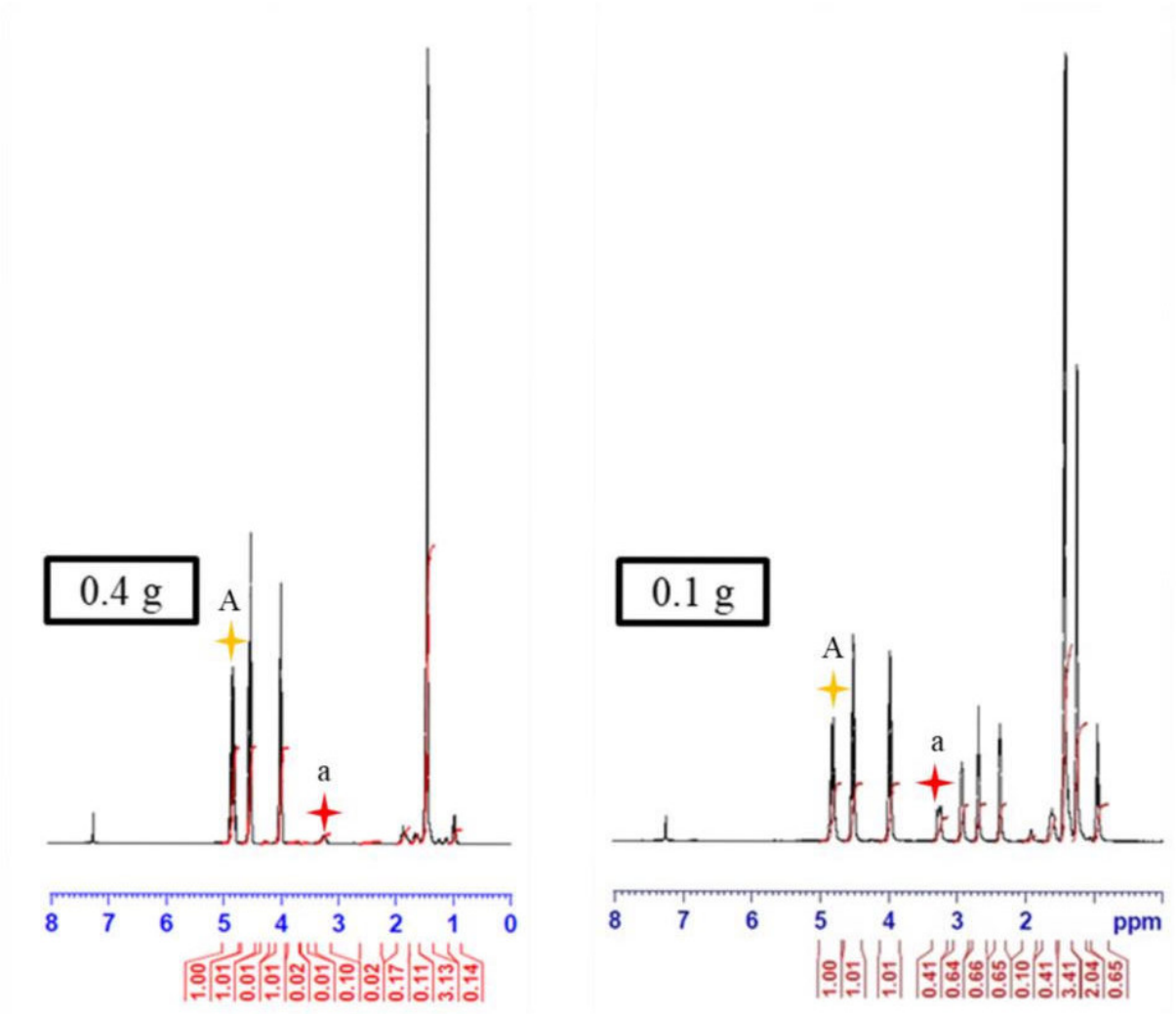

Figure A 8. ^{1}H NMR Analysis: Catalytic performance towards conversion (left image): Catalyst loading is 0.4 g; (right image): Catalyst loading is 0.1 g; A: PC (A) and a: PO (a)

References

[1] Z. Zięba, J. Dąbrowska, M. Marschalko, J. Pinto, M. Mrówczyńska, A. Leśniak, A. Petrovski, J.K. Kazak, Built Environment Challenges Due to Climate Change, IOP Conference Series: Earth and Environmental Science, 609 (2020) 012061.

[2] W.C. Lu, Greenhouse Gas Emissions, Energy Consumption and Economic Growth: A Panel Cointegration Analysis for 16 Asian Countries, Int J Environ Res Public Health, 14 (2017).

[3] M.M. Rahman, S.M. Rahman, M. Shafiullah, M.A. Hasan, U. Gazder, A. Al Mamun, U. Mansoor, M.T. Kashifi, O. Reshi, M. Arifuzzaman, M.K. Islam, F.S. Al-Ismail, Energy Demand of the Road Transport Sector of Saudi Arabia—Application of a Causality-Based Machine Learning Model to Ensure Sustainable Environment, in: Sustainability, 2022.

[4] C. Le Quéré, R.M. Andrew, P. Friedlingstein, S. Sitch, J. Hauck, J. Pongratz, P.A. Pickers, J.I. Korsbakken, G.P. Peters, J.G. Canadell, A. Arneth, V.K. Arora, L. Barbero, A. Bastos, L. Bopp, F. Chevallier, L.P. Chini, P. Ciais, S.C. Doney, T. Gkritzalis, D.S. Goll, I. Harris, V. Haverd, F.M. Hoffman, M. Hoppema, R.A. Houghton, G. Hurtt, T. Ilyina, A.K. Jain, T. Johannessen, C.D. Jones, E. Kato, R.F. Keeling, K.K. Goldewijk, P. Landschützer, N. Lefèvre, S. Lienert, Z. Liu, D. Lombardozzi, N. Metzl, D.R. Munro, J.E.M.S. Nabel, S. Nakaoka, C. Neill, A. Olsen, T. Ono, P. Patra, A. Peregon, W. Peters, P. Peylin, B. Pfeil, D. Pierrot, B. Poulter, G. Rehder, L. Resplandy, E. Robertson, M. Rocher, C. Rödenbeck, U. Schuster, J. Schwinger, R. Séférian, I. Skjelvan, T. Steinhoff, A. Sutton, P.P. Tans, H. Tian, B. Tilbrook, F.N. Tubiello, I.T. van der Laan-Luijkx, G.R. van der Werf, N. Viovy, A.P. Walker, A.J. Wiltshire, R. Wright, S. Zaehle, B. Zheng, Global Carbon Budget 2018, Earth Syst. Sci. Data, 10 (2018) 2141-2194.

[5] Z. Liu, Z. Deng, G. He, H. Wang, X. Zhang, J. Lin, Y. Qi, X. Liang, Challenges and opportunities for carbon neutrality in China, Nature Reviews Earth & Environment, 3 (2022) 141-155.

[6] S. Li, T. Hu, Y. Xu, J. Wang, R. Chu, Z. Yin, F. Mo, L. Zhu, A review on flocculation as an efficient method to harvest energy microalgae: Mechanisms, performances, influencing factors and perspectives, Renewable and Sustainable Energy Reviews, 131 (2020) 110005.

[7] I. Ghiat, T. Al-Ansari, A review of carbon capture and utilisation as a CO_2 abatement opportunity within the EWF nexus, Journal of CO2 Utilization, 45 (2021) 101432.

[8] N. Noorani, B. Barzegar, A. Mehrdad, H. Aghdasinia, S.J. Peighambardoust, H. Kazemian, CO_2 capture in activated pyrolytic coke/metal oxide nanoparticle composites, Colloids and Surfaces A: Physicochemical and Engineering Aspects, 679 (2023) 132554.

[9] R. Sabouni, H. Kazemian, S. Rohani, Carbon dioxide capturing technologies: a review focusing on metal organic framework materials (MOFs), Environmental Science and Pollution Research, 21 (2014) 5427-5449.

[10] R. Sabouni, H. Kazemian, S. Rohani, Carbon dioxide adsorption in microwave-synthesized metal organic framework CPM-5: Equilibrium and kinetics study, Microporous and Mesoporous Materials, 175 (2013) 85-91.

[11] A. Schoedel, Z. Ji, O.M. Yaghi, The role of metal–organic frameworks in a carbon-neutral energy cycle, Nature Energy, 1 (2016) 1-13.

[12] C. Jiang, X. Wang, K. Lu, W. Jiang, H. Xu, X. Wei, Z. Wang, Y. Ouyang, F. Dai, From layered structure to 8-fold interpenetrated MOF with enhanced selective adsorption of C_2H_2/CH_4 and CO_2/CH_4, Journal of Solid State Chemistry, 307 (2022) 122881.

[13] L. Li, J. He, W. Xu, K. Zhang, T. Xing, Z. Li, D. Zhen, B. Xiong, Z. Ge, X. Zhang, High CO_2 separation performance on a metal–organic framework composed of nano-cages lined with an ultra-high density of dual-side open metal sites, Materials Advances, 3 (2022) 493-497.

[14] S. Qadir, Y. Gu, S. Ali, D. Li, S. Zhao, S. Wang, H. Xu, S. Wang, A thermally stable isoquinoline based ultra-microporous metal-organic framework for CH_4 separation from coal mine methane, Chemical Engineering Journal, 428 (2022) 131136.

[15] S. Venet, F. Plantier, C. Miqueu, A. Shahtalebi, R. Brown, T. Pigot, P. Bordat, CO_2 capture and CO_2/CH_4 separation by silicas with controlled porosity and functionality, Microporous and Mesoporous Materials, 332 (2022) 111651.
[16] R. Sabouni, H. Kazemian, S. Rohani, A novel combined manufacturing technique for rapid production of IRMOF-1 using ultrasound and microwave energies, Chemical Engineering Journal, 165 (2010) 966-973.
[17] M.H. Aboonasr Shiraz, E. Rehl, H. Kazemian, J. Liu, Durable Lithium/Selenium Batteries Enabled by the Integration of MOF-Derived Porous Carbon and Alucone Coating, Nanomaterials, 11 (2021) 1976.
[18] M. Bahri, F. Haghighat, H. Kazemian, S. Rohani, A comparative study on metal organic frameworks for indoor environment application: Adsorption evaluation, Chemical Engineering Journal, 313 (2017) 711-723.
[19] J.-B. Lin, T.T. Nguyen, R. Vaidhyanathan, J. Burner, J.M. Taylor, H. Durekova, F. Akhtar, R.K. Mah, O. Ghaffari-Nik, S. Marx, A scalable metal-organic framework as a durable physisorbent for carbon dioxide capture, Science, 374 (2021) 1464-1469.
[20] M. Lalehchini, M.M. Alavi Nikje, A. Mohajeri, H. Kazemian, A Green, Economic Method for Bench-Scale Activation of a MIL-101(Cr) Nanoadsorbent, Industrial & Engineering Chemistry Research, 62 (2023) 598-609.
[21] H.C. Gulbalkan, Z.P. Haslak, C. Altintas, A. Uzun, S. Keskin, Assessing CH_4/N_2 separation potential of MOFs, COFs, IL/MOF, MOF/Polymer, and COF/Polymer composites, Chemical Engineering Journal, 428 (2022) 131239.
[22] L.-C. Lin, D. Paik, J. Kim, Understanding gas adsorption in MOF-5/graphene oxide composite materials, Physical Chemistry Chemical Physics, 19 (2017) 11639-11644.
[23] H. Djahaniani, N. Ghavidel, H. Kazemian, Green and facile synthesis of lignin/HKUST-1 as a novel hybrid biopolymer metal-organic-framework for a pH-controlled drug release system, International Journal of Biological Macromolecules, 242 (2023) 124627.
[24] C. Wu, K. Zhang, H. Wang, Y. Fan, S. Zhang, S. He, F. Wang, Y. Tao, X. Zhao, Y.-B. Zhang, Enhancing the gas separation selectivity of mixed-matrix membranes using a dual-interfacial engineering approach, Journal of the American Chemical Society, 142 (2020) 18503-18512.
[25] Y. Chen, D. Lv, J. Wu, J. Xiao, H. Xi, Q. Xia, Z. Li, A new MOF-505@ GO composite with high selectivity for CO_2/CH_4 and CO_2/N_2 separation, Chemical Engineering Journal, 308 (2017) 1065-1072.
[26] T. Wu, N. Prasetya, K. Li, Recent advances in aluminium-based metal-organic frameworks (MOF) and its membrane applications, Journal of Membrane Science, 615 (2020) 118493.
[27] M.F. Ghazvini, M. Vahedi, S.N. Nobar, F. Sabouri, Investigation of the MOF adsorbents and the gas adsorptive separation mechanisms, Journal of Environmental Chemical Engineering, 9 (2021) 104790.
[28] A. Khan, M.A. Qyyum, H. Saulat, R. Ahmad, X. Peng, M. Lee, Metal–organic frameworks for biogas upgrading: recent advancements, challenges, and future recommendations, Applied Materials Today, 22 (2021) 100925.
[29] S. Dai, A. Tissot, C. Serre, Recent progresses in metal–organic frameworks based core–shell composites, Advanced Energy Materials, 12 (2022) 2100061.
[30] V. Muthukumaraswamy Rangaraj, M.A. Wahab, K.S.K. Reddy, G. Kakosimos, O. Abdalla, E.P. Favvas, D. Reinalda, F. Geuzebroek, A. Abdala, G.N. Karanikolos, Metal organic framework—based mixed matrix membranes for carbon dioxide separation: recent advances and future directions, Frontiers in Chemistry, 8 (2020) 534.
[31] J. Liu, C. Chen, K. Zhang, L. Zhang, Applications of metal–organic framework composites in CO_2 capture and conversion, Chinese Chemical Letters, 32 (2021) 649-659.
[32] Y. Shi, B. Liang, R.-B. Lin, C. Zhang, B. Chen, Gas separation via hybrid metal–organic framework/polymer membranes, Trends in Chemistry, 2 (2020) 254-269.

[33] B. Szczęśniak, J. Choma, M. Jaroniec, Gas adsorption properties of hybrid graphene-MOF materials, Journal of colloid and interface science, 514 (2018) 801-813.
[34] Q. Al-Naddaf, H. Thakkar, F. Rezaei, Novel zeolite-5A@ MOF-74 composite adsorbents with core–shell structure for H_2 purification, ACS applied materials & interfaces, 10 (2018) 29656-29666.
[35] G. Sargazi, D. Afzali, A. Mostafavi, H. Kazemian, A novel composite derived from a metal organic framework immobilized within electrospun nanofibrous polymers: An efficient methane adsorbent, Applied Organometallic Chemistry, 34 (2020) e5448.
[36] H. Kazemian, S. Rohani, Microwave Synthesis Porous Zeolitic Metal–Organic Framework Materials, in: Microwave Engineering of Nanomaterials, Jenny Stanford Publishing, 2016, pp. 245-278.
[37] Q. Al-Naddaf, A.A. Rownaghi, F. Rezaei, Multicomponent adsorptive separation of CO_2, CO, CH_4, N_2, and H2 over core-shell zeolite-5A@ MOF-74 composite adsorbents, Chemical Engineering Journal, 384 (2020) 123251.
[38] F. Yang, J. Wu, X. Zhu, T. Ge, R. Wang, Enhanced stability and hydrophobicity of LiX@ ZIF-8 composite synthesized environmental friendly for CO_2 capture in highly humid flue gas, Chemical Engineering Journal, 410 (2021) 128322.
[39] K.L. Tate, S. Li, M. Yu, M.A. Carreon, Zeolite adsorbent-MOF layered nanovalves for CH_4 storage, Adsorption, 23 (2017) 19-24.
[40] H. Roohollahi, H. Zeinalzadeh, H. Kazemian, Recent Advances in Adsorption and Separation of Methane and Carbon Dioxide Greenhouse Gases Using Metal–Organic Framework-Based Composites, Industrial & Engineering Chemistry Research, 61 (2022) 10555-10586.
[41] N.E. Tari, A. Tadjarodi, J. Tamnanloo, S. Fatemi, One pot microwave synthesis of MCM-41/Cu based MOF composite with improved CO_2 adsorption and selectivity, Microporous and Mesoporous Materials, 231 (2016) 154-162.
[42] F. Gao, Y. Li, Z. Bian, J. Hu, H. Liu, Dynamic hydrophobic hindrance effect of zeolite@ zeolitic imidazolate framework composites for CO_2 capture in the presence of water, Journal of Materials Chemistry A, 3 (2015) 8091-8097.
[43] J.H. Aldrich, S.M. Rousselo, M.L. Yang, S.M. Araiza, F. Tian, Adsorptive separation of methane from carbon dioxide by zeolite@ ZIF composite, Energy & Fuels, 33 (2018) 348-355.
[44] H. Roohollahi, R. Halladj, H. Ebrahimi, S. Askari, An overall experimental analysis: Effects of synthetic parameters on the degree of order of mesochannels in nano-sized Al-MCM-41, Heteroatom Chemistry, 29 (2018) e21457.
[45] C.-P. Ye, R.-N. Wang, X. Gao, W.-Y. Li, CO_2 Capture Performance of supported phosphonium dual amine-functionalized ionic liquids@ MCM-41, Energy & Fuels, 34 (2020) 14379-14387.
[46] H. Roohollahi, R. Halladj, S. Askari, F. Yaripour, SAPO-34/AlMCM-41, as a novel hierarchical nanocomposite: preparation, characterization and investigation of synthesis factors using response surface methodology, Journal of Solid State Chemistry, 262 (2018) 273-281.
[47] N.E. Tari, A. Tadjarodi, J. Tamnanloo, S. Fatemi, Synthesis and property modification of MCM-41 composited with Cu(BDC) MOF for improvement of CO_2 adsorption Selectivity, Journal of CO2 Utilization, 14 (2016) 126-134.
[48] C. Chen, N. Feng, Q. Guo, Z. Li, X. Li, J. Ding, L. Wang, H. Wan, G. Guan, Template-directed fabrication of MIL-101(Cr)/mesoporous silica composite: Layer-packed structure and enhanced performance for CO_2 capture, Journal of Colloid and Interface Science, 513 (2018) 891-902.
[49] S. Sorribas, B. Zornoza, P. Serra-Crespo, J. Gascon, F. Kapteijn, C. Téllez, J. Coronas, Synthesis and gas adsorption properties of mesoporous silica-NH2-MIL-53(Al) core–shell spheres, Microporous and Mesoporous Materials, 225 (2016) 116-121.
[50] A. Chakraborty, S. Laha, K. Kamali, C. Narayana, M. Eswaramoorthy, T.K. Maji, In Situ Growth of Self-Assembled ZIF-8–Aminoclay Nanocomposites with Enhanced Surface Area and CO_2 Uptake, Inorganic Chemistry, 56 (2017) 9426-9435.

[51] Q. Zhao, Q. Yan, J. Tian, H. Wang, Low-carbon economy transformation performance evaluation and spatial trends in China: a provincial aspect, Greenhouse Gases: Science and Technology, 9 (2019) 886-904.
[52] T.A. Kurniawan, M.H.D. Othman, X. Liang, H.H. Goh, P. Gikas, K.-K. Chong, K.W. Chew, Challenges and opportunities for biochar to promote circular economy and carbon neutrality, Journal of Environmental Management, 332 (2023) 117429.
[53] Y. Tan, H. Yang, J. Cheng, J. Hu, G. Tian, X. Yu, Preparation of hydrogen from metals and water without CO_2 emissions, International Journal of Hydrogen Energy, 47 (2022) 38134-38154.
[54] F. Qureshi, M. Yusuf, H. Kamyab, D.-V.N. Vo, S. Chelliapan, S.-W. Joo, Y. Vasseghian, Latest eco-friendly avenues on hydrogen production towards a circular bioeconomy: Currents challenges, innovative insights, and future perspectives, Renewable and Sustainable Energy Reviews, 168 (2022) 112916.
[55] P. Challa, G. Paleti, V.R. Madduluri, S.B. Gadamani, R. Pothu, D.R. Burri, R. Boddula, V. Perugopu, S.R.R. Kamaraju, Trends in Emission and Utilization of CO_2: Sustainable Feedstock in the Synthesis of Value-Added Fine Chemicals, Catalysis Surveys from Asia, 26 (2022) 80-91.
[56] T. Sakakura, J.-C. Choi, H. Yasuda, Transformation of Carbon Dioxide, Chemical Reviews, 107 (2007) 2365-2387.
[57] M. Chehrazi, B.K. Moghadas, A review on CO_2 capture with chilled ammonia and CO_2 utilization in urea plant, Journal of CO_2 Utilization, 61 (2022) 102030.
[58] M. Aresta, A. Dibenedetto, Utilisation of CO_2 as a chemical feedstock: opportunities and challenges, Dalton Transactions, (2007) 2975-2992.
[59] Y. Wu, J. Xu, K. Mumford, G.W. Stevens, W. Fei, Y. Wang, Recent advances in carbon dioxide capture and utilization with amines and ionic liquids, Green Chemical Engineering, 1 (2020) 16-32.
[60] M. Takht Ravanchi, S. Sahebdelfar, Carbon dioxide capture and utilization in petrochemical industry: potentials and challenges, Applied Petrochemical Research, 4 (2014) 63-77.
[61] M.D. Burkart, N. Hazari, C.L. Tway, E.L. Zeitler, Opportunities and Challenges for Catalysis in Carbon Dioxide Utilization, ACS Catalysis, 9 (2019) 7937-7956.
[62] I.K.M. Yu, D.C.W. Tsang, A.C.K. Yip, A.J. Hunt, J. Sherwood, J. Shang, H. Song, Y.S. Ok, C.S. Poon, Propylene carbonate and γ-valerolactone as green solvents enhance Sn(iv)-catalysed hydroxymethylfurfural (HMF) production from bread waste, Green Chemistry, 20 (2018) 2064-2074.
[63] R.C. Thakur, A. Sharma, R. Sharma, H. Kaur, A comparative analysis of volumetric, viscometric and conductometric properties of Triethylmethylammonium Tetrafluoroborate (TEMABF4) and Tetraethylammonium Tetrafluoroborate (TEABF4) in pure propylene carbonate (PC) and binary aqueous propylene carbonate solvents, Journal of Molecular Liquids, 374 (2023) 121244.
[64] S.-R. Zhang, Y. Fu, H. Lv, G.-P. Cao, Hydrotalcite-calcined derivatives doped by zinc: A nucleophile-modified multifunctional catalyst for synthesis of propylene carbonate by cycloaddition, Catalysis Communications, 175 (2023) 106603.
[65] R. Kumar, K. Sadeghi, J. Jang, J. Seo, Mechanical, chemical, and bio-recycling of biodegradable plastics: A review, Science of The Total Environment, 882 (2023) 163446.
[66] C.S. Funari, D. Rinaldo, V.S. Bolzani, R. Verpoorte, Reaction of the Phytochemistry Community to Green Chemistry: Insights Obtained Since 1990, Journal of Natural Products, 86 (2023) 440-459.
[67] D. Prat, A. Wells, J. Hayler, H. Sneddon, C.R. McElroy, S. Abou-Shehada, P.J. Dunn, CHEM21 selection guide of classical- and less classical-solvents, Green Chemistry, 18 (2016) 288-296.
[68] L. Guo, K.J. Lamb, M. North, Recent developments in organocatalysed transformations of epoxides and carbon dioxide into cyclic carbonates, Green Chemistry, 23 (2021) 77-118.
[69] E. Pérez-Mayoral, M. Godino-Ojer, I. Matos, M. Bernardo, Opportunities from Metal Organic Frameworks to Develop Porous Carbons Catalysts Involved in Fine Chemical Synthesis, Catalysts, 13 (2023) 541.

[70] Z. Yuan, M.R. Eden, R. Gani, Toward the Development and Deployment of Large-Scale Carbon Dioxide Capture and Conversion Processes, Industrial & Engineering Chemistry Research, 55 (2016) 3383-3419.
[71] F.N. Al-Rowaili, U. Zahid, S. Onaizi, M. Khaled, A. Jamal, E.M. Al-Mutairi, A review for Metal-Organic Frameworks (MOFs) utilization in capture and conversion of carbon dioxide into valuable products, Journal of CO_2 Utilization, 53 (2021) 101715.
[72] J. Gandara-Loe, L. Pastor-Perez, L.F. Bobadilla, J.A. Odriozola, T.R. Reina, Understanding the opportunities of metal–organic frameworks (MOFs) for CO_2 capture and gas-phase CO_2 conversion processes: a comprehensive overview, Reaction Chemistry & Engineering, 6 (2021) 787-814.
[73] B.R. Pimentel, A. Parulkar, E.-k. Zhou, N.A. Brunelli, R.P. Lively, Zeolitic Imidazolate Frameworks: Next-Generation Materials for Energy-Efficient Gas Separations, ChemSusChem, 7 (2014) 3202-3240.
[74] A. Modak, P. Bhanja, S. Dutta, B. Chowdhury, A. Bhaumik, Catalytic reduction of CO_2 into fuels and fine chemicals, Green Chemistry, 22 (2020) 4002-4033.
[75] F. Valizadeh Harzand, S.N. Mousavi Nejad, A. Babapoor, S.M. Mousavi, S.A. Hashemi, A. Gholami, W.-H. Chiang, M.G. Buonomenna, C.W. Lai, Recent Advances in Metal-Organic Framework (MOF) Asymmetric Membranes/Composites for Biomedical Applications, Symmetry, 15 (2023) 403.
[76] Introduction to Metal–Organic Frameworks, Chemical Reviews, 112 (2012) 673-674.
[77] N.L. Rosi, J. Kim, M. Eddaoudi, B. Chen, M. O'Keeffe, O.M. Yaghi, Rod Packings and Metal−Organic Frameworks Constructed from Rod-Shaped Secondary Building Units, Journal of the American Chemical Society, 127 (2005) 1504-1518.
[78] W.-Y. Gao, Y. Chen, Y. Niu, K. Williams, L. Cash, P.J. Perez, L. Wojtas, J. Cai, Y.-S. Chen, S. Ma, Crystal Engineering of an nbo Topology Metal–Organic Framework for Chemical Fixation of CO_2 under Ambient Conditions, Angewandte Chemie International Edition, 53 (2014) 2615-2619.
[79] G. Cai, P. Yan, L. Zhang, H.-C. Zhou, H.-L. Jiang, Metal–Organic Framework-Based Hierarchically Porous Materials: Synthesis and Applications, Chemical Reviews, 121 (2021) 12278-12326.
[80] S.S.A. Shah, T. Najam, M. Wen, S.-Q. Zang, A. Waseem, H.-L. Jiang, Metal–Organic Framework-Based Electrocatalysts for CO_2 Reduction, Small Structures, 3 (2022) 2100090.
[81] I.I. Alkhatib, C. Garlisi, M. Pagliaro, K. Al-Ali, G. Palmisano, Metal-organic frameworks for photocatalytic CO_2 reduction under visible radiation: A review of strategies and applications, Catalysis Today, 340 (2020) 209-224.
[82] S.E.M. Elhenawy, M. Khraisheh, F. AlMomani, G. Walker, Metal-Organic Frameworks as a Platform for CO_2 Capture and Chemical Processes: Adsorption, Membrane Separation, Catalytic-Conversion, and Electrochemical Reduction of CO_2, Catalysts, 10 (2020) 1293.
[83] A. Zanon, F. Verpoort, Metals@ZIFs: Catalytic applications and size selective catalysis, Coordination Chemistry Reviews, 353 (2017) 201-222.
[84] Y.V. Kaneti, S. Dutta, M.S.A. Hossain, M.J.A. Shiddiky, K.-L. Tung, F.-K. Shieh, C.-K. Tsung, K.C.-W. Wu, Y. Yamauchi, Strategies for Improving the Functionality of Zeolitic Imidazolate Frameworks: Tailoring Nanoarchitectures for Functional Applications, Advanced Materials, 29 (2017) 1700213.
[85] R. Ahmad, U.A. Khan, N. Iqbal, T. Noor, Zeolitic imidazolate framework (ZIF)-derived porous carbon materials for supercapacitors: an overview, RSC Advances, 10 (2020) 43733-43750.
[86] S. Daliran, A.R. Oveisi, Y. Peng, A. López-Magano, M. Khajeh, R. Mas-Ballesté, J. Alemán, R. Luque, H. Garcia, Metal–organic framework (MOF)-, covalent-organic framework (COF)-, and porous-organic polymers (POP)-catalyzed selective C–H bond activation and functionalization reactions, Chemical Society Reviews, 51 (2022) 7810-7882.

[87] Y. Sun, N. Zhang, Y. Yue, J. Xiao, X. Huang, A. Ishag, Recent advances in the application of zeolitic imidazolate frameworks (ZIFs) in environmental remediation: a review, Environmental Science: Nano, 9 (2022) 4069-4092.
[88] M. Almáši, Chapter 28 - Current development in MOFs for hydrogen storage: a mechanistic investigation, in: R.K. Gupta, T.A. Nguyen, G. Yasin (Eds.) Metal-Organic Framework-Based Nanomaterials for Energy Conversion and Storage, Elsevier, 2022, pp. 631-661.
[89] S. Dutta, J. Kim, P.-H. Hsieh, Y.-S. Hsu, Y.V. Kaneti, F.-K. Shieh, Y. Yamauchi, K.C.-W. Wu, Nanoarchitectonics of Biofunctionalized Metal–Organic Frameworks with Biological Macromolecules and Living Cells, Small Methods, 3 (2019) 1900213.
[90] Y. Liu, Q. Wang, J. Zhang, J. Ding, Y. Cheng, T. Wang, J. Li, F. Hu, H.B. Yang, B. Liu, Recent Advances in Carbon-Supported Noble-Metal Electrocatalysts for Hydrogen Evolution Reaction: Syntheses, Structures, and Properties, Advanced Energy Materials, 12 (2022) 2200928.
[91] S. Kumar, S. Jain, M. Nehra, N. Dilbaghi, G. Marrazza, K.-H. Kim, Green synthesis of metal–organic frameworks: A state-of-the-art review of potential environmental and medical applications, Coordination Chemistry Reviews, 420 (2020) 213407.
[92] D. Crawford, J. Casaban, R. Haydon, N. Giri, T. McNally, S.L. James, Synthesis by extrusion: continuous, large-scale preparation of MOFs using little or no solvent, Chemical Science, 6 (2015) 1645-1649.
[93] J. Yang, J. Wang, B. Hou, X. Huang, T. Wang, Y. Bao, H. Hao, Porous hydrogen-bonded organic frameworks (HOFs): From design to potential applications, Chemical Engineering Journal, 399 (2020) 125873.
[94] P. Tomkins, M. Ranocchiari, J.A. van Bokhoven, Direct Conversion of Methane to Methanol under Mild Conditions over Cu-Zeolites and beyond, Accounts of Chemical Research, 50 (2017) 418-425.
[95] N.N.R. Ahmad, C.P. Leo, A.W. Mohammad, A.L. Ahmad, Modification of gas selective SAPO zeolites using imidazolium ionic liquid to develop polysulfone mixed matrix membrane for CO_2 gas separation, Microporous and Mesoporous Materials, 244 (2017) 21-30.
[96] M. Ahmed, A. Sakthivel, Preparation of cyclic carbonate via cycloaddition of CO_2 on epoxide using amine-functionalized SAPO-34 as catalyst, Journal of CO_2 Utilization, 22 (2017) 392-399.
[97] Z. Xie, M. Zhu, A. Nambo, J.B. Jasinski, M.A. Carreon, Microwave-assisted synthesized SAPO-56 as a catalyst in the conversion of CO_2 to cyclic carbonates, Dalton Transactions, 42 (2013) 6732-6735.
[98] X. Liu, N. Yan, L. Wang, C. Ma, P. Guo, P. Tian, G. Cao, Z. Liu, Landscape of AlPO-based structures and compositions in the database of zeolite structures, Microporous and Mesoporous Materials, 280 (2019) 105-115.
[99] R.B. Rostami, M. Ghavipour, R.M. Behbahani, A. Aghajafari, Improvement of SAPO-34 performance in MTO reaction by utilizing mixed-template catalyst synthesis method, Journal of Natural Gas Science and Engineering, 20 (2014) 312-318.
[100] M. Ghavipour, A.S. Mehr, Y. Wang, R.M. Behbahani, S. Hajimirzaee, K. Bahrami, Investigating the mixing sequence and the Si content in SAPO-34 synthesis for selective conversion of methanol to light olefins using morpholine &/ TEAOH templates, RSC Advances, 6 (2016) 17583-17594.
[101] J.A. Castro-Osma, C. Alonso-Moreno, A. Lara-Sánchez, J. Martínez, M. North, A. Otero, Synthesis of cyclic carbonates catalysed by aluminium heteroscorpionate complexes, Catalysis Science & Technology, 4 (2014) 1674-1684.
[102] B. Ebadinezhad, M. Haghighi, Texture evolution of mesoporous SAPO-34 via a hard-templating sono-hydrothermal method for biodiesel production: Influence of carbon materials on nanocatalyst design, Applied Catalysis A: General, 595 (2020) 117486.

[103] Y. Wang, X. Liu, M. Wang, X. Wang, W. Ma, J. Li, Facile synthesis of CDs@ZIF-8 nanocomposites as excellent peroxidase mimics for colorimetric detection of H2O2 and glutathione, Sensors and Actuators B: Chemical, 329 (2021) 129115.
[104] X. Luo, J. Guo, P. Chang, H. Qian, F. Pei, W. Wang, K. Miao, S. Guo, G. Feng, ZSM-5@MCM-41 composite porous materials with a core-shell structure: Adjustment of mesoporous orientation basing on interfacial electrostatic interactions and their application in selective aromatics transport, Separation and Purification Technology, 239 (2020) 116516.
[105] A.K. Gupta, N. Guha, S. Krishnan, P. Mathur, D.K. Rai, A Three-Dimensional Cu(II)-MOF with Lewis acid−base dual functional sites for Chemical Fixation of CO_2 via Cyclic Carbonate Synthesis, Journal of CO2 Utilization, 39 (2020) 101173.
[106] D.G. Boer, J. Langerak, P.P. Pescarmona, Zeolites as Selective Adsorbents for CO_2 Separation, ACS Applied Energy Materials, (2023).
[107] B. Wang, P. Rui, X. Cai, X. Xie, W. Liao, Y. Luo, X. Shu, Insights into the methanol to olefins (MTO) performance of SAPO-34 under the stripper conditions of fluid catalytic cracking (FCC), Microporous and Mesoporous Materials, 345 (2022) 112244.
[108] K.-R. Oh, H. Lee, G.-N. Yun, C. Yoo, J.W. Yoon, A. Awad, H.-W. Jeong, Y.K. Hwang, Fabrication of Hierarchical, Porous, Bimetallic, Zeolitic Imidazolate Frameworks with the Incorporation of Square Planar Pd and Its Catalytic Application, ACS Applied Materials & Interfaces, 15 (2023) 9296-9306.
[109] A.K. Singh, R. Yadav, A. Sakthivel, Synthesis, characterization, and catalytic application of mesoporous SAPO-34 (MESO-SAPO-34) molecular sieves, Microporous and mesoporous materials, 181 (2013) 166-174.
[110] Y. Zhang, Y. Jia, Synthesis of zeolitic imidazolate framework-8 on polyester fiber for PM 2.5 removal, RSC advances, 8 (2018) 31471-31477.
[111] K.M. Bhin, J. Tharun, K.R. Roshan, D.-W. Kim, Y. Chung, D.-W. Park, Catalytic performance of zeolitic imidazolate framework ZIF-95 for the solventless synthesis of cyclic carbonates from CO_2 and epoxides, Journal of CO_2 Utilization, 17 (2017) 112-118.
[112] V.I. Isaeva, M.N. Timofeeva, I.A. Lukoyanov, E.Y. Gerasimov, V.N. Panchenko, V.V. Chernyshev, L.M. Glukhov, L.M. Kustov, Novel MOF catalysts based on calix [4] arene for the synthesis of propylene carbonate from propylene oxide and CO_2, Journal of CO_2 Utilization, 66 (2022) 102262.
[113] Y.-F. Lin, K.-W. Huang, B.-T. Ko, K.-Y.A. Lin, Bifunctional ZIF-78 heterogeneous catalyst with dual Lewis acidic and basic sites for carbon dioxide fixation via cyclic carbonate synthesis, Journal of CO_2 Utilization, 22 (2017) 178-183.
[114] H. Su, Y. Yan, J.-N. Zhang, W. Yan, CO_2 captured by silicoaluminophosphate (SAPO) zeotypes, Sustainable Chemistry for Climate Action, (2023) 100022.
[115] X. Wang, H. Chen, M. Zhang, C. Wang, Y. Wang, P. Bai, L. Li, W. Yan, Organic template-free synthesis of K-SAPO-34 zeolite for efficient CO_2 separation, Fuel, 338 (2023) 127233.
[116] V.I. Isaeva, M.N. Timofeeva, I.A. Lukoyanov, E.Y. Gerasimov, V.N. Panchenko, V.V. Chernyshev, L.M. Glukhov, L.M. Kustov, Novel MOF catalysts based on calix[4]arene for the synthesis of propylene carbonate from propylene oxide and CO2, Journal of CO2 Utilization, 66 (2022) 102262.
[117] H. Ryu, R. Roshan, M.-I. Kim, D.-W. Kim, M. Selvaraj, D.-W. Park, Cycloaddition of carbon dioxide with propylene oxide using zeolitic imidazolate framework ZIF-23 as a catalyst, Korean Journal of Chemical Engineering, 34 (2017) 928-934.
[118] M.N. Timofeeva, I.A. Lukoyanov, V.N. Panchenko, K.I. Shefer, M.S. Mel'gunov, B.N. Bhadra, S.H. Jhung, Tuning the catalytic properties for cycloaddition of CO_2 to propylene oxide on zeolitic-imidazolate frameworks through variation of structure and chemical composition, Molecular Catalysis, 529 (2022) 112530.

[119] X. Li, A.K. Cheetham, J. Jiang, CO2 cycloaddition with propylene oxide to form propylene carbonate on a copper metal-organic framework: A density functional theory study, Molecular Catalysis, 463 (2019) 37-44.